

Article

Asymmetric Quantum Multicast Network Coding: Asymmetric Optimal Cloning over Quantum Networks

Yuichi Hirota and Masaki Owari *

Department of Computer Science, Faculty of Informatics, Shizuoka University, Hamamatsu 432-8011, Japan; yu1.16ta@gmail.com

* Correspondence: masakiowari@inf.shizuoka.ac.jp

Abstract: Multicasting of quantum states is an essential feature of quantum internet. Since the noncloning theorem prohibits perfect cloning of an unknown quantum state, an appropriate protocol may depend on the purpose of the multicast. In this paper, we treat the multicasting of a single copy of an unknown state over a quantum network with free classical communication. We especially focus on protocols *exactly* multicasting an asymmetric optimal universal clone. Hence, these protocols are optimal and universal in terms of mean fidelity between input and output states, but the fidelities can depend on target nodes. Among these protocols, a protocol spending smaller communication resources is preferable. Here, we construct such a protocol attaining the min-cut of the network described as follows. Two (three) asymmetric optimal clones of an input state are created at a source node. Then, the state is divided into classical information and a compressed quantum state. The state is sent to two (three) target nodes using the quantum network coding. Finally, the asymmetric clones are reconstructed using LOCC with a small amount of entanglement shared among the target nodes and the classical information sent from the source node.

Keywords: quantum information; quantum communication; quantum network; universal cloning; network coding; entanglement



Citation: Hirota, Y.; Owari, M. Asymmetric Quantum Multicast Network Coding: Asymmetric Optimal Cloning over Quantum Networks. *Appl. Sci.* **2022**, *12*, 6163. <https://doi.org/10.3390/app12126163>

Academic Editors: Nikola Paunković and André Souto

Received: 7 April 2022

Accepted: 14 June 2022

Published: 17 June 2022

Publisher's Note: MDPI stays neutral with regard to jurisdictional claims in published maps and institutional affiliations.



Copyright: © 2022 by the authors. Licensee MDPI, Basel, Switzerland. This article is an open access article distributed under the terms and conditions of the Creative Commons Attribution (CC BY) license (<https://creativecommons.org/licenses/by/4.0/>).

1. Introduction

In recent years, rapid progress has been made in the research and development of standalone quantum computers [1], both in terms of software and hardware, to the point where it is debated whether quantum computational supremacy has achieved [2–4]. In the near future, standalone quantum computers are expected to show innovative performance in various fields, such as machine learning [5–9] and computational chemistry [10–14]. On the other hand, it is known that much quantum information processing, including various different types of quantum cryptography such as quantum public-key cryptography [15], quantum blind computation [16,17], and quantum money [18,19] cannot be realized on standalone quantum computers but only on quantum networks [20], where a quantum network of a large size is called quantum internet [21,22]. Thus, recently, quantum network has been intensively studied both theoretically [23–29] and experimentally [30,31].

Theoretical research for improving the throughput of quantum networks started from the study of quantum repeaters aiming to share a maximally entangled state between end vertices of a quantum network represented by a path graph [32,33]. After an enormous amount of research in this direction (see [20] and references therein), the ultimate limit for sharing a maximally entangled state between a given pair of nodes on a quantum network was finally derived by Pirandola et al. [24,26]. On the other hand, since multiple users may simultaneously communicate with each other, it is also important to study multiparty communication protocol on a quantum network. In general, the problem of finding a better multiparty communication protocol on a quantum network is much more complicated than a problem of a two-party communication protocol. First, even on the classical network, there are many different types of multiparty communication. Simple examples of

multiparty communication may be multiple-unicast communication and multicast communication, where the definitions of these schemes are given later in this introduction. However, in general, an arbitrary type of communication among multiple parties can be considered [34], and we need to optimize the communication protocol depending on the type. Furthermore, there is an additional problem with multiparty communication on quantum networks. As is well known, “a class of maximally entangled states” is not unique [35] in a multipartite system, which is represented by the incomparability of GHZ states and W states under stochastic local operation and classical communication (SLOCC) [36]. This fact suggests that depending on our purpose, we need to use a different multiparty protocol to share a different type of states. In other words, we cannot discuss the optimality of the multiparty protocol before we determine what type of states we want to share.

In classical information theory, a technique called network coding is known to be useful to improve throughput of various different multiparty communication schemes when there is a bottleneck on a network. Here, network coding is a technique of applying nontrivial operations to the bitstream at intermediate nodes [37–39]. The method of network coding can be also applied to quantum networks, and quantum information processing on a quantum network that utilizes methods of network coding is called “a quantum network coding” [40]. There has been a considerable amount of research on quantum network coding, which tries to improve the throughput of a quantum network in various situations [41–57]. Recently, it has been presented that quantum network coding can improve the security of a quantum network [58–61] and reduce decoherence effect [62]. Furthermore, it is useful for quantum repeater networks [63,64] as well as for distributed quantum computation [65]. Moreover, a simple quantum network code has been experimentally demonstrated [66,67]. Although many studies have considered network coding on noisy classical networks in classical information theory, almost all the studies of quantum network coding consider noise-free quantum networks. This is because quantum network coding is regarded as a protocol implemented on a layer on which the errors have been already corrected. Hence, in this study, we consider noise-free quantum networks.

In classical network coding, the majority of the studies have focused on multicast communication, where a single source node transmits the same information to multiple target nodes on a network [37,38]. The left-hand side of Figure 1 shows the network coding for the butterfly network. This is one of the simplest examples of classical multicast network coding. Another type of network coding is called multiple-unicast network coding. Here, there are k pairs of source and target nodes $(s_0, t_0), \dots, (s_{k-1}, t_{k-1})$ on the network, and each source node s_i independently transmits a message to the corresponding target node t_i for all i [68]. The modified version of the butterfly network in the right-hand side of Figure 1 is one of the simplest examples of classical multiple-unicast network coding.

Most of the research on quantum network coding considered multiple-unicast communication, i.e., multiple-unicast quantum network coding, where each source node transmits a quantum state (instead of a classical message) to the corresponding target node [41,43,45,46,53,58–61,63,64]. The most important results are those of Kobayashi et al. If classical information (or measurement results) can be freely sent among the nodes on a quantum network, Kobayashi et al. gave a canonical procedure for constructing a quantum multiple-unicast network code from a given classical multiple-unicast network code. Here, the quantum network for the quantum code and the classical network for the classical code must be represented by the same graph [43,46].

They showed that this problem can be considered as a generalization of classical multicast communication and presented protocols using network coding to probabilistically achieve the above goal on the multiple-unicast butterfly network given in the right figure of Figure 1. Although the protocols of Shi et al., Kobayashi et al., and Xu et al. can be considered as generalizations of classical multicast network coding to quantum networks, rigorously speaking, the goal of their protocols is not exactly to achieve a multicast of a quantum state.

Recently, Pan et al. proposed a new multicast protocol using quantum network coding [57]. The purpose of the protocol is to probabilistically send an exact copy or an exact orthogonal complement of a known qubit state from a source node to multiple target nodes on a quantum network. Because the sender knows the state, this protocol does not contradict the no-cloning theorem [69]. On the other hand, this task is trivial when free classical communication is allowed. Hence, they consider the situation where each channel on the quantum network can send either one qubit or two classical bits in a single session of the protocol; that is, classical communication is restricted in their problem setting. They give an efficient protocol to achieve this goal on the multicast butterfly network given in the left figure of Figure 1 and also on the extended butterfly network.

In this paper, we consider a yet different problem setting on multicast on the quantum network. As we have already mentioned, perfect multicast of an unknown state is impossible. Nevertheless, imperfect multicast of an unknown quantum state is still possible. When we restrict ourselves to imperfect multicast of a quantum state through noiseless quantum channels, the problem of multicast of an unknown quantum state reduces to a problem of cloning an unknown quantum state. This problem is called quantum approximate cloning [70,71] and has been intensively studied both theoretically [72–85] and experimentally [86–91].

The performance of a cloning protocol is normally measured in terms of the fidelity between an unknown input state and an output clone. When this fidelity does not depend on an input state, the protocol is called universal cloning. Among them, a protocol achieving the maximum fidelity is called optimal universal cloning [70,71]. Here, we need to add the following remark. When M output clones ρ_i ($i = 1 \cdots M$) of an input unknown state, $|\psi\rangle$ are created by a cloning protocol. We need to treat M independent fidelities $F_i := \langle \psi | \rho_i | \psi \rangle$ and cannot straightforwardly define an optimal protocol. One way to resolve this problem is to add a constraint that all the clones are equivalent, that is, $\rho_i = \rho_j$ for all i and j . This immediately leads $F_i = F_j$ for all i and j , and the optimal universal cloning satisfying this condition is called symmetric optimal universal quantum cloning. On the other hand, when we do not use the constraint of symmetry, we need to define a weight w_i satisfying $w_i \geq 0$ and $\sum_i w_i = 1$ and a weighted mean fidelity $\bar{F} := \sum_i w_i F_i$. The universal cloning which is optimal in terms of \bar{F} is called asymmetric optimal universal quantum cloning. By the definition, symmetric optimal universal cloning is a special case of asymmetric optimal universal quantum cloning such that the weight $w_i = 1/M$ for all i .

In the viewpoint of multiparty communication, optimal universal quantum cloning is nothing but a multicast quantum channel that is optimal in terms of fidelity. Therefore, when we consider a quantum network communication, sending an optimal universal quantum clone (UQC) from a single source node to multiple target nodes is a multicast network communication that is optimal in terms of fidelity. Furthermore, this problem may be considered one of the most natural quantum extensions of classical multicast network coding. Hence, our research problem to study in which condition this communication task is achievable is information-theoretically important. Furthermore, it is known that quantum approximate cloning is useful for several information processing tasks including eavesdropping on quantum key distribution protocols [92–96], broadcasting quantum coherence [97], and multiple-unicast quantum network coding over the butterfly network without classical communication [40]. This fact strongly suggests that our research problem is practically important as well.

Based on this idea, Owari et al. constructed a protocol to exactly share a symmetric optimal UQC of an input state on the target nodes under the conditions that classical information can be sent freely among nodes on a quantum network and that a small amount of entanglement is shared on target nodes at the beginning of the protocol [49,50]. They also gave a protocol to approximately share a symmetric optimal UQC without entanglement shared among target nodes [48]. We further note that although the references [48–50] are written in Japanese, their English version is now planned to be written [98].

In this paper, we focus on extending Owari et al.'s results [49,50] to asymmetric optimal universal quantum cloning [75–85], which is a generalization of symmetric optimal universal quantum cloning. Thus, we construct a protocol to efficiently and *exactly* multicast an asymmetric optimal clone of a q^r -dimensional input quantum state from one source node to two (three) target nodes, where q is assumed to be a prime power.

Our problem setting is given by the following four assumptions, which are almost in common with those used in [49,50]:

- The noise-free quantum network can be described by an undirected graph G with one source node and two (three) target nodes.
- Each quantum channel on the quantum network can transmit one q -dimensional quantum system in a single session.
- Measurement results (or classical information) can be sent freely from one node to another node on the quantum network.
- A small amount of entanglement that does not scale with q , is shared among the target nodes. The amount of entanglement is at most 2 ebit for two target nodes, and at most $(2 + 4 \log_2 3)$ ebit for the case of three target nodes.

Under these assumptions, we prove that multicasting of $1 \rightarrow 2$ ($1 \rightarrow 3$) asymmetric optimal UQCs of a q^r -dimensional state is possible, if there exists a classical solvable linear multicast network code with source rate r for a noise-free classical network described by an acyclic directed graph G' , where G is an undirected underlying graph of G' . Using the max-flow and min-cut theorem of multicast network coding [37,38], for sufficiently large q , this sufficient condition for the existence of a classical network code on G' can be replaced by the condition that the minimum-cut between the source node s and a target node t_i is no less than r for all i .

An outline of our protocol is as follows:

- We create two (three) asymmetric optimal UQCs of an input state with an ancilla system at a source node.
- We measure the ancilla system and send the measurement outcomes to the target nodes.
- We compress the whole d^2 (d^3)-dimensional system into a d -dimensional system.
- We transmit the resulting state to two (three) target nodes using Kobayashi et al.'s multicast quantum network coding [44]. As a result, a GHZ-type state is shared among target nodes.
- We reconstruct the asymmetric optimal UQCs of the input state from the GHZ-type state using LOCC with a small amount of entanglement among the target nodes and the measurement outcomes sent from the source node.

Using the above protocol, we can multicast asymmetric optimal clones from one source node to two (three) target nodes (Figure 2). Here, we note that although the above outline of our protocol is almost the same as the protocol of Owari et al. of symmetric optimal UQCs, the detail of each part is completely different.

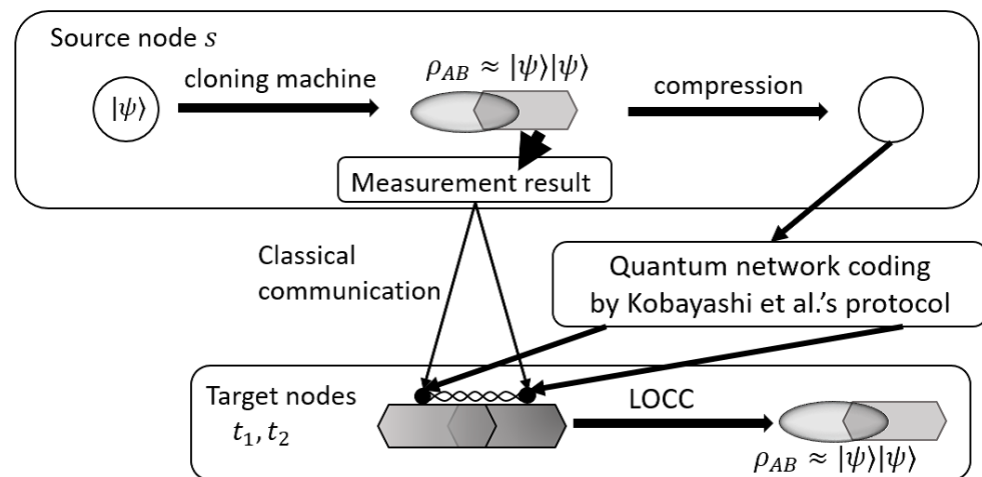


Figure 2. Schematic diagram of a protocol for multicasting asymmetric optimal UQCs from one source node to two target nodes. The asymmetric optimal cloning protocol for the input state $|\psi\rangle$ is implemented at the source node. The resulting state is compressed into a d -dimensional system and transmitted to the two target nodes using the quantum multicast network coding protocol of Kobayashi et al. [44]. Finally, the asymmetric optimal clones of the input state are reconstructed by LOCC on target nodes with the help of a small amount of entanglement.

To see the efficiency of our protocol, it is convenient to consider the multicast butterfly network given on the left-hand side of Figure 1. When each edge corresponds to a q -dimensional noiseless quantum channel and the target nodes t_0 and t_1 share 2 ebit, our protocol distributes asymmetric optimal QCMs of q^2 -dimensional input states. On the other hand, we can easily see that a conventional protocol without network coding based on entanglement swapping (or quantum repeater) only distributes asymmetric optimal QCMs of q -dimensional input states at most. Hence, the rate of our protocol is double that of the conventional protocol. We further show that the above protocol can be used for efficient preparation of quantum asymmetric telecloning [99,100] over a quantum network.

The rest of the paper is organized as follows: We explain the asymmetric optimal universal quantum cloning and the quantum multicast network coding protocol of Kobayashi et al. in Section 2. We present all the results in Section 3, where a protocol for multicasting $1 \rightarrow 2$ asymmetric optimal clones is given in Section 3.1. We also present a protocol for multicasting $1 \rightarrow 3$ asymmetric optimal clones in Section 3.2. Finally, we give a discussion and summary in Section 4.

2. Materials and Methods

Asymmetric optimal universal quantum cloning, classical linear multicast network coding, and the multicast quantum network coding protocol of Kobayashi et al. are all important in our protocol. In this section, we explain optimal asymmetric universal quantum cloning in Section 2.1. Then, classical linear multicast network coding and the multicast quantum network coding protocol of Kobayashi et al. are presented in Sections 2.2 and 2.3, respectively.

2.1. Optimal Asymmetric Quantum Universal Cloning Machine

The no-cloning theorem states that quantum mechanics prohibits a quantum operation that makes perfect copies of an unknown quantum state [69]. That is, there is no quantum channel (or a completely positive and trace preserving map) $\varepsilon : \mathfrak{B}(\mathcal{H}) \rightarrow \mathfrak{B}(\mathcal{H}^{\otimes 2})$ satisfying $\varepsilon(\rho) = \rho \otimes \rho$ for all pure states ρ on a Hilbert space \mathcal{H} , where $\mathfrak{B}(\mathcal{H})$ is a space of all linear operators on the Hilbert space \mathcal{H} . This immediately leads to the impossibility of a perfect multicast of an unknown quantum state. On the other hand, quantum mechanics does not completely prohibit approximate cloning of a quantum state. Thus, there may exist a quantum channel $\varepsilon : \mathfrak{B}(\mathcal{H}) \rightarrow \mathfrak{B}(\mathcal{H}^{\otimes 2})$ such that $\text{Tr}_2 \varepsilon(\rho)$ and $\text{Tr}_1 \varepsilon(\rho)$ are close to ρ for

an arbitrary pure state ρ , where Tr_i is the partial trace of the i th subsystem. Hence, many studies have focused on quantum protocols to make an approximate copy of unknown states (so-called quantum cloning machines) [72–85].

In general, a quantum cloning machine (QCM) that produces N approximate clones based on M copies of a given quantum state $|\psi\rangle \in \mathcal{H}$ is a quantum channel ε from $\mathfrak{B}(\mathcal{H}^{\otimes M})$ to $\mathfrak{B}(\mathcal{H}^{\otimes N})$. Suppose that ρ_i is a reduced density matrix of the output state on the i th subsystem: $\rho_i = \text{Tr}_{-i} \varepsilon(|\psi\rangle\langle\psi|^{\otimes M})$, where Tr_{-i} is a partial trace of all subsystems except the i th subsystem. Since the purpose of a QCM is to make ρ_i as closed as the input state $|\psi\rangle\langle\psi|$, the performance of a QCM can be described by the output fidelity F_i between ρ_i and $|\psi\rangle\langle\psi|$:

$$F_i = \langle\psi|\rho_i|\psi\rangle, \quad (i = 1, \dots, M). \tag{2}$$

A QCM is called universal if F_i does not depend on the input state $|\psi\rangle$. Furthermore, a universal QCM (UQCM) is called symmetric if the all clones are the same: $\rho_i = \rho_j$ for all i and j . A UQCM that is not symmetric is asymmetric. Since the output states of an asymmetric UQCM satisfy $\rho_i \neq \rho_j$, the output fidelity F_i also depends on i . Thus, to discuss the optimality of an asymmetric UQCM, we need to define a weight $\{w_i\}_{i=1}^M$ satisfying $w_i \geq 0$ and $\sum_{i=1}^M w_i = 1$. Then, the mean output fidelity \bar{F} of an asymmetric UQCM ε with respect to the weight $\{w_i\}_{i=1}^M$ is defined by

$$\bar{F} := \sum_i^M w_i F_i. \tag{3}$$

For a given weight $\{w_i\}_{i=1}^M$, an asymmetric UQCM that attains the optimum of the mean output fidelity \bar{F} is called an asymmetric optimal UQCM w.r.t $\{w_i\}$.

For existing results on asymmetric optimal UQCM, we refer to [71,84]. Here, we only give known facts on asymmetric optimal UQCM that are necessary for our research. First, we give an optimal asymmetric UQCM with $M = 1$ and $N = 2$ (we call this protocol a $1 \rightarrow 2$ optimal asymmetric UQCM). This protocol uses three systems: A , B , and M , whose Hilbert spaces are \mathcal{H}_A , \mathcal{H}_B , and \mathcal{H}_M , respectively. Here, \mathcal{H}_A works as an input system and the first output system, \mathcal{H}_B is the second output system, and \mathcal{H}_M is an ancilla system. The dimensions of all three systems are the same, and we denote this dimension as d ; that is, $\dim \mathcal{H}_A = \dim \mathcal{H}_B = \dim \mathcal{H}_M =: d$. Then, for an input state $|\psi\rangle$ on system A , a $1 \rightarrow 2$ optimal asymmetric UQCM is given by an isometry $U_{1 \rightarrow 2}^{(a,b)}$ from \mathcal{H}_A to $\mathcal{H}_A \otimes \mathcal{H}_B \otimes \mathcal{H}_M$ satisfying [78]:

$$U_{1 \rightarrow 2}^{(a,b)}|\psi\rangle_A = a|\psi\rangle_A|\Phi_d^+\rangle_{BM} + b|\psi\rangle_B|\Phi_d^+\rangle_{AM}. \tag{4}$$

where $|\Phi_d^+\rangle$ is a standard d -dimensional maximally entangled state:

$$|\Phi_d^+\rangle := \frac{1}{\sqrt{d}} \sum_{k=0}^{d-1} |k\rangle|k\rangle, \tag{5}$$

and a and b are positive real parameters satisfying

$$a^2 + b^2 + \frac{2ab}{d} = 1. \tag{6}$$

Note that in order to simplify the formulas, the parameters a, b are often used instead of the weight $\{w_i\}_{i=1}^2$ in the definition of the $1 \rightarrow 2$ optimal asymmetric UQCM. Using $U_{1 \rightarrow 2}^{(a,b)}$ defined above, the optimal asymmetric UQCM $\varepsilon_{1 \rightarrow 2}^{(a,b)}$ is

$$\varepsilon_{1 \rightarrow 2}^{(a,b)}(|\psi\rangle\langle\psi|) := \text{Tr}_M(U_{1 \rightarrow 2}|\psi\rangle\langle\psi|_A U_{1 \rightarrow 2}^\dagger). \tag{7}$$

The reduced density matrices of the output states can be written as

$$\begin{aligned} \rho_A &:= \text{Tr}_B \varepsilon_{1 \rightarrow 2}^{(a,b)}(|\psi\rangle\langle\psi|) = (1 - b^2)|\psi\rangle\langle\psi| + b^2 \frac{I}{d} \\ \rho_B &:= \text{Tr}_A \varepsilon_{1 \rightarrow 2}^{(a,b)}(|\psi\rangle\langle\psi|) = (1 - a^2)|\psi\rangle\langle\psi| + a^2 \frac{I}{d}. \end{aligned} \tag{8}$$

Thus, the fidelity of the reduced density matrices, which have been proved to be optimum [78], is given by

$$\begin{aligned} F_A &:= \langle\psi|\text{Tr}_B\left(\varepsilon_{1 \rightarrow 2}^{(a,b)}(|\psi\rangle\langle\psi|)\right)|\psi\rangle = 1 - b^2 \frac{d-1}{d}, \\ F_B &:= \langle\psi|\text{Tr}_A\left(\varepsilon_{1 \rightarrow 2}^{(a,b)}(|\psi\rangle\langle\psi|)\right)|\psi\rangle = 1 - a^2 \frac{d-1}{d}, \end{aligned} \tag{9}$$

where I is an identity operator on a d -dimensional system. The well-known formula $F_A = F_B = \frac{d+3}{2(d+1)}$ of the fidelity of an optimal symmetric UQCM is derived from the above equations by substituting $a = b$ [71].

Next, we give an optimal asymmetric UQCM with $M = 1$ and $N = 3$ (we call this protocol the $1 \rightarrow 3$ optimal asymmetric UQCM). This protocol use five systems $A, B, C, R,$ and S whose Hilbert spaces are $\mathcal{H}_A, \mathcal{H}_B, \mathcal{H}_C, \mathcal{H}_R,$ and $\mathcal{H}_S,$ respectively. Here, \mathcal{H}_A is an input system that is also the first output system. \mathcal{H}_B and \mathcal{H}_C are the second and third output systems, respectively. \mathcal{H}_R and \mathcal{H}_S are ancilla systems. The dimensions of all systems are the same, which we denote as d . For an input state $|\psi\rangle$ on system $A, 1 \rightarrow 3$ optimal asymmetric UQCM is given by an isometry $U_{1 \rightarrow 3}^{(\alpha,\beta,\gamma)}$ from \mathcal{H}_A to $\mathcal{H}_A \otimes \mathcal{H}_B \otimes \mathcal{H}_C \otimes \mathcal{H}_R \otimes \mathcal{H}_S$ satisfying the following equation:

$$\begin{aligned} U_{1 \rightarrow 3}^{(\alpha,\beta,\gamma)}|\psi\rangle &= \sqrt{\frac{d}{2d+2}}[\alpha|\psi\rangle_A(|\Phi_d^+\rangle_{BR}|\Phi_d^+\rangle_{CS} + |\Phi_d^+\rangle_{BS}|\Phi_d^+\rangle_{CR}) \\ &\quad + \beta|\psi\rangle_B(|\Phi_d^+\rangle_{AR}|\Phi_d^+\rangle_{CS} + |\Phi_d^+\rangle_{AS}|\Phi_d^+\rangle_{CR}) \\ &\quad + \gamma|\psi\rangle_C(|\Phi_d^+\rangle_{AR}|\Phi_d^+\rangle_{BS} + |\Phi_d^+\rangle_{AS}|\Phi_d^+\rangle_{BR})]. \end{aligned} \tag{10}$$

Here, α, β, γ are non-negative real parameters which are used instead of the weight $\{w_i\}_{i=1}^3$ and satisfy the following constraint [71,79,80]:

$$\alpha^2 + \beta^2 + \gamma^2 + \frac{2}{d}(\alpha\beta + \beta\gamma + \alpha\gamma) = 1. \tag{11}$$

In terms of $U_{ABCRS},$ a $1 \rightarrow 3$ optimal asymmetric UQCM $\varepsilon_{1 \rightarrow 3}^{(\alpha,\beta,\gamma)}$ can be written as:

$$\varepsilon_{1 \rightarrow 3}^{(\alpha,\beta,\gamma)}(|\psi\rangle\langle\psi|) := \text{Tr}_{RS}\left(U_{1 \rightarrow 3}^{(\alpha,\beta,\gamma)}|\psi\rangle\langle\psi|_A U_{1 \rightarrow 3}^{(\alpha,\beta,\gamma)\dagger}\right). \tag{12}$$

The fidelities between an input state and each reduced density matrix, which were proved to be optimum [71,79,80], are given as follows:

$$\begin{aligned} F_A &= 1 - \frac{d-1}{d}\left(\beta^2 + \gamma^2 + \frac{2\beta\gamma}{d+1}\right), \\ F_B &= 1 - \frac{d-1}{d}\left(\alpha^2 + \gamma^2 + \frac{2\alpha\gamma}{d+1}\right), \\ F_C &= 1 - \frac{d-1}{d}\left(\alpha^2 + \beta^2 + \frac{2\alpha\beta}{d+1}\right). \end{aligned} \tag{13}$$

We refer [79] for the figure depicting behavior of $F_A, F_B,$ and F_C with respect to α, β and $\gamma.$

2.2. Classical Multicast Network Coding

Since our protocol uses the protocol of Kobayashi et al. as a subroutine and since the protocol of Kobayashi et al. is based on a classical linear multicast network code, we introduce classical linear multicast network coding in this subsection. A detailed description of classical multicast network coding can be found in standard textbooks of network coding [37,38].

A classical network is represented by a directed graph $G' = (V, E')$, where a vertex $v \in V$ represents a node of the network and an edge $e \in E'$ represents a noiseless classical channel. In this paper, we assume that G' is *acyclic*. There exist a source node $s \in V$ and N target nodes $t_1, \dots, t_N \in V$ on the network. A node that is neither a source node nor a target node is called an intermediate node. In a single session of a classical multicast network coding, an alphabet on the finite field \mathbb{F}_q is sent from node u to node v if $(u, v) \in E'$, where the order of \mathbb{F}_q is a prime power q . Since G' is an acyclic directed graph, a natural partial ordering can be defined on E' . This partial ordering is generated by the condition that $(u, v), (v, w) \in E' \implies (u, v) \prec (v, w)$. The order of transmissions of classical information can be determined by this partial ordering. That is, an edge $e \in E'$ transmits an alphabet after all edges $e' \in E'$ satisfying $e' \prec e$ have transmitted alphabets. We assume that there is no incoming edge to the source node s and that there is no outgoing edge from any target node. Hence, all edges whose tail node is the source node s are a local minimum, and all edges whose head node is a target node are a local maximum under the partial ordering. We further assume that all edges whose tail node is not the source node s are not a local minimum and that all edges whose head node is not a target node are not a local maximum. This is because the edges that do not satisfy these conditions are useless for our purpose.

A classical linear multicast network code over \mathbb{F}_q on G' consists of a set of linear maps $\{f_e\}_{e \in E'}$. At the beginning of a session, an input message $\vec{x} := (x_1, \dots, x_r) \in \mathbb{F}_q^r$ is chosen on the source node s , where r is the source rate of the classical multicast network code. Suppose e is an outgoing edge of v . At the first step of the network coding, an alphabet y_e transmitted through the edge e is chosen as a linear combination of x_1, \dots, x_r . In other words, in terms of a linear function $f_e : \mathbb{F}_q^r \rightarrow \mathbb{F}_q$, y_e can be written as

$$y_e := f_e(\vec{x}) = f_e(x_1, \dots, x_r). \tag{14}$$

After calculating y_e , y_e is transmitted through e . After all edges outgoing from the source node s transmitted an alphabet, all intermediate nodes transmit alphabet in the order determined by the partial ordering as follows: Suppose an intermediate node v on the network has m incoming edges and e is an outgoing edge from v . After all transmissions of m incoming edges to v have finished, the node v has m -alphabets $y_j \in \mathbb{F}_q$ ($j = 1, \dots, m$), where y_j is an alphabet sent through the j th incoming edge. Then, an alphabet y_e transmitted through the edge e is chosen as a linear combination of y_1, \dots, y_m . In other words, there exists a linear function $f_e : \mathbb{F}_q^m \rightarrow \mathbb{F}_q$ such that

$$y_e := f_e(y_1, \dots, y_m). \tag{15}$$

After the calculation, y_e is transmitted through e .

Suppose a target node t_i has m_i incoming edges. Then, after all edges have transmitted an alphabet, the target node t_i has m_i -alphabets $y_j^{(i)} \in \mathbb{F}_q$ ($j = 1, \dots, m_i$), where $y_j^{(i)}$ is an alphabet sent through the j th incoming edge to t_i . A classical linear multicast network code $\{f_e\}_{e \in E'}$ is called *solvable* if there exists a set of decoding operations $\{g_i\}_{i=1}^N$ such that $g_i : \mathbb{F}_q^{m_i} \rightarrow \mathbb{F}_q^r$ satisfies the following equation for all i :

$$\vec{x} = g_i(y_1^{(i)}, \dots, y_{m_i}^{(i)}), \tag{16}$$

where $\vec{x} \in \mathbb{F}_q^r$ is the input message. If a classical linear multicast network code is solvable, any decoding operation g_i can be chosen as a linear map.

There is a necessary and sufficient condition for the existence of a classical linear multicast network code [37,38]. Suppose that C_i is the size of the minimum cut between s and t_i . Then, there exists a classical linear multicast code with source rate r on G' over a sufficiently large field \mathbb{F}_q if and only if $C_i \geq r$ for all i . This is nothing but a generalization of the famous max-flow min-cut theorem to a multicast network communication.

2.3. Quantum Multicast Network Coding

In this subsection, we review the protocol of Kobayashi et al. [44]. First, we give a problem setting for multicast quantum network coding that is common between our protocol and the protocol of Kobayashi et al. A quantum network is described by an undirected graph $G = (V, E)$, where V represents a set of nodes and E represents a set of quantum channels. There exist a source node $s \in V$ and N target nodes $t_1, \dots, t_N \in V$ on the network. In a single session, any quantum channel $(u, v) \in E$ can send a q -dimensional quantum system \mathcal{H}_e just once either from u to v , or from v to u , where q is assumed to be a prime power. Furthermore, any quantum operations can be implemented on any node $v \in V$, and measurement outcomes (or classical information) can be freely sent among nodes. At the beginning of a session, a single copy of input state $|\psi\rangle$ is given on the source node s . Here, the reason a quantum channel is represented by an undirected edge is that the direction of a quantum channel can be effectively reversed by quantum teleportation under the condition of free classical communication [45].

The purpose of both protocols is to multicast an input state $|\psi\rangle$ from the source node to all target nodes in a single session. Here, we should note that the meaning of “multicast” in the protocol of Kobayashi et al. is different from that in our protocol. As we have explained in the introduction, the purpose of our protocol is to construct optimal asymmetric universal clones among target nodes for a given q^r -dimensional input state $|\psi\rangle = \sum_{j=0}^{q^r-1} \alpha_j |j\rangle \in \mathcal{H}_s$ on a source node, where \mathcal{H}_s is a q^r -dimensional input space. In other words, we consider multicast quantum network coding with source rate r . On the other hand, the purpose of the protocol of Kobayashi et al. is to construct a GHZ-type state $\sum_{j=0}^{q^r-1} \alpha_j |j\rangle_1 \otimes \dots \otimes |j\rangle_N$ among target nodes, where the i th local system is on the i th target node.

Both the protocol of Kobayashi et al. and our protocol are constructed under the assumption that there exists a solvable classical linear multicast network code $\{f_e\}_{e \in E'}$ with source rate r on an acyclic directed graph $G' = (V, E')$ over a finite field \mathbb{F}_q , where G is an undirected underlying graph of G' . In other words, G can be derived by replacing all directed edges on G' by undirected edges. Using this replacement, a directed edge $e' \in E'$ is naturally mapped to an undirected $e \in E$, and this map is a bijection. Hence, in the following part of this subsection, we will not distinguish e' from e and will write e' as e .

The protocol of Kobayashi et al. imitates a classical linear multicast network code $\{f_e\}_{e \in E'}$ and corresponding decoding operations $\{g_i\}_{i=1}^N$ by unitary operators. Each linear map f_e is imitated by a unitary operator U_e , and each recovery operator g_i is imitated by a unitary operator V_i , where U_e and V_i are defined as follows: Since $\dim \mathcal{H}_s = q^r$, due to the bijection between $\{0, 1 \dots q^r - 1\}$ and \mathbb{F}_q^r , an input state $|\psi\rangle \in \mathcal{H}_s$ can be written as $|\psi\rangle = \sum_{\vec{x} \in \mathbb{F}_q^r} \alpha_{\vec{x}} |\vec{x}\rangle$. For an outgoing edge e from the source node s , a unitary operator U_e on $\mathcal{H}_s \otimes \mathcal{H}_e$ is defined by means of $f_e : \mathbb{F}_q^r \rightarrow \mathbb{F}_q$ as

$$U_e := \sum_{\vec{x} \in \mathbb{F}_q^r, \vec{y} \in \mathbb{F}_q} |\vec{x}\rangle \langle \vec{x}|_s \otimes |\vec{y} + f_e(\vec{x})\rangle \langle \vec{y}|_e, \tag{17}$$

where \mathcal{H}_e is a Hilbert space transmitted through e . Suppose $In(e)$ is a set of all incoming edges of v , where v is a tail node of e , and suppose $\mathcal{H}_{In(e)} := \otimes_{e' \in In(e)} \mathcal{H}_{e'}$. Then, for an outgoing edge e from an intermediate node v , a unitary operator U_e on $\mathcal{H}_{In(e)} \otimes \mathcal{H}_e$ is defined by means of $f_e : \mathbb{F}_q^{|In(e)|} \rightarrow \mathbb{F}_q$ as

$$U_e := \sum_{\vec{y} \in \mathbb{F}_q^{|In(e)|}, \vec{y}_e \in \mathbb{F}_q} |\vec{y}\rangle \langle \vec{y}|_{In(e)} \otimes |\vec{y}_e + f_e(\vec{y})\rangle \langle \vec{y}_e|_e. \tag{18}$$

Suppose \mathcal{V}_i is a q^r -dimensional output Hilbert space on a target node t_i . A unitary operator V_i on $\mathcal{H}_{In(t_i)} \otimes \mathcal{V}_i$ is defined by means of the decoding operation $g_i : \mathbb{F}_q^{|In(t_i)|} \rightarrow \mathbb{F}_q^r$ as

$$V_i := \sum_{\vec{y} \in \mathbb{F}_q^{|In(t_i)|}, \vec{x} \in \mathbb{F}_q^r} |\vec{y}\rangle \langle \vec{y}|_{In(t_i)} \otimes |\vec{x} + g_i(\vec{y})\rangle \langle \vec{x}|. \tag{19}$$

The quantum multicast network coding protocol of Kobayashi et al. is shown in Protocol 1.

Protocol 1 The quantum multicast network coding protocol of Kobayashi et al.

Step 1: Initialization

At the beginning, the source node s has an unknown initial state $|\psi\rangle$ on \mathcal{H}_s . Each node $v \in V$ prepares $|0\rangle$ on \mathcal{H}_e for an edge $e \in E$ whose tail node is v . For all i satisfying $1 \leq i \leq m$, a target node t_i prepares $|0\rangle$ on \mathcal{V}_i .

Step 2: Transmission

First, for all edges $e \in E'$ whose tail node is the source node, the source node operates the unitary operator U_e on $\mathcal{H}_s \otimes \mathcal{H}_e$ and sends \mathcal{H}_e to the head node of e . Second, all intermediate nodes operate in the order defined by the natural partial ordering on E' as follows: After an intermediate node v has received Hilbert spaces from all edges whose head node is v , for all edges $e \in E'$ whose tail node is v , node v operates the unitary operator U_e on $\mathcal{H}_{In(e)} \otimes \mathcal{H}_e$ and sends \mathcal{H}_e to the head node of e . Finally, after all edges have transmitted Hilbert spaces, for all i satisfying $1 \leq i \leq m$, target node t_i operates the unitary operator V_i on $\mathcal{H}_{In(t_i)} \otimes \mathcal{V}_i$.

Step 3: Measurement on Fourier basis

The source node s measures the Hilbert space \mathcal{H}_s in the Fourier basis and sends the measurement outcome to all the terminal nodes t_i . For all edges $e \in E'$, the head node of e measures the Hilbert space \mathcal{H}_e in the Fourier basis and sends the measurement outcome to all terminal nodes t_i .

Step 4: Recovery

All terminal nodes t_i operate $Z(c_1) \otimes \dots \otimes Z(c_r)$ on \mathcal{V}_i . Here, $\{c_k\}_{k=1}^r$ is a set of natural numbers that can be determined from the measurement outcomes received in step 3, the classical linear multicast network code $\{f_e\}_{e \in E'}$ and the decoding operators $\{g_i\}_{i=1}^m$ [44].

In Step 3 of Protocol 1, the Fourier basis of $\{|\tilde{z}\rangle\}_{z \in \mathbb{F}_q} \subset \mathcal{H}_e$ of the computational basis $\{|x\rangle\}_{x \in \mathbb{F}_q} \subset \mathcal{H}_e$ is defined as

$$|\tilde{z}\rangle := \sum_{x \in \mathbb{F}_q} \omega^{\text{Tr}xz} |x\rangle,$$

where $\omega := \exp(-2\pi i/p)$. Here, $\text{Tr} z$ represents the element $\text{Tr} M_z \in \mathbb{F}_p$, where M_z is the matrix representation of the multiplication map $x \mapsto zx$. Here, we note that the finite field \mathbb{F}_q can be identified with the vector space \mathbb{F}_p^t , where t is the degree of the algebraic extension of \mathbb{F}_q . For further details, see [101], Section 8.1.2. We also define the generalized Pauli operators $Z(t)$ as $Z(t) := \sum_{x \in \mathbb{F}_q} \omega^{\text{Tr}xt} |x\rangle \langle x|$.

3. Results

In this section, we give all results of this paper. We give results for $1 \rightarrow 2$ and $1 \rightarrow 3$ asymmetric UQCs in the Sections 3.1 and 3.2, respectively.

3.1. $1 \rightarrow 2$ Asymmetric UQC Multicast Protocol

In this subsection, we present a new protocol that multicasts optimal asymmetric UQCs from the source node s to two target nodes t_1 and t_2 on a quantum network. We present the protocol in Section 3.1.1 and prove that it creates optimal asymmetric UQCs in Section 3.1.2.

3.1.1. 1 → 2 Quantum Multicast Protocol

In this sub-subsection, we present the protocol for multicasting 1 → 2 asymmetric optimal UQCs of an input quantum state from the source node s to two target nodes t_1 and t_2 .

As we have explained in Section 2.3, the problem settings for the protocol of Kobayashi et al. and our protocol are essentially the same, and only their purposes are different. Here, we summarize the problem setting of our quantum multicast network coding: A quantum network is described by an *undirected* graph $G = (V, E)$. There exist a source node $s \in V$ and N target nodes $t_1, \dots, t_N \in V$ on the network. In this subsection, since we consider multicasting 1 → 2 asymmetric UQCs, we set $N = 2$. In a single session, any quantum channel $(u, v) \in E$ can send a q -dimensional quantum system \mathcal{H}_e just once, either from u to v or from v to u , where q is assumed to be a prime power. Furthermore, any quantum operations can be implemented on any node $v \in V$, and measurement outcomes can be freely sent among nodes. At the beginning of a session, a single copy of input state $|\psi\rangle$ is given on the source node s .

Under these problem settings, the purpose of our protocol is to construct optimal asymmetric universal clones given by Equation (7) between target nodes t_1 and t_2 for a given d -dimensional unknown input state $|\psi\rangle = \sum_{j=0}^d \alpha_j |j\rangle \in \mathcal{H}_s$ on a source node, where \mathcal{H}_s is a d -dimensional input space. In other words, we consider multicast communication protocols that are optimal in terms of fidelity. Thus, our research problem is to construct a protocol with a smaller communication cost under the above condition. We assume $d = q^r$. In other words, we consider multicast quantum network coding with source rate r . Here, note that since we assumed q is a prime power, d is also a prime power.

For this purpose, we use two additional assumptions: The first assumption is the same assumption that Kobayashi et al. used. That is, we assume that there exists a solvable classical linear multicast network code $\{f_e\}_{e \in E'}$ with source rate r on an acyclic directed graph $G' = (V, E')$ over a finite field \mathbb{F}_q , where G is an undirected underlying graph of G' . Hence, we can use the quantum multicast network coding protocol of Kobayashi et al. with source rate r on this quantum network G . We further assume that at most 2 ebits of entanglement resource are shared between target node t_1 and t_2 . Hence, the amount of this entanglement resource is constant with respect to the dimension d of the input state and is negligible for large d in comparison to d .

Before we present the protocol, we define the unitary operators used in it. Pauli operators X_d and Z_d are defined as

$$X_d := \sum_{k=0}^{d-1} |k \oplus 1\rangle \langle k|, \quad Z_d := \sum_{k=0}^{d-1} \omega^k |k\rangle \langle k|, \tag{20}$$

where $\omega := e^{\frac{2\pi i}{d}}$. In the following part of the paper, unitary operators defined on $\mathbb{C}^d \otimes \mathbb{C}^d$ and $\mathbb{C}^d \otimes \mathbb{C}^d \otimes \mathbb{C}^d$ are called bipartite and tripartite unitary operators, respectively. $Y^{(r)}$ is defined as a bipartite unitary operator satisfying

$$\begin{aligned} Y^{(r)}(\cos \eta |jr\rangle + \sin \eta |rj\rangle) &= |jr\rangle, & Y^{(r)}|rr\rangle &= |rr\rangle, \\ Y^{(r)}(\sin \eta |jr\rangle - \cos \eta |rj\rangle) &= |rj\rangle \end{aligned} \tag{21}$$

for all $j \in \{0, \dots, d - 1\}$ satisfying $j \neq r$, and

$$Y^{(r)}|ij\rangle = |ij\rangle \tag{22}$$

for all $i, j \in \{0, \dots, d - 1\}$ satisfying $i, j \neq r$, where η is defined by

$$\cos \eta = \frac{a}{\sqrt{1 - \frac{2ab}{d}}} \quad \text{and} \quad \sin \eta = \frac{b}{\sqrt{1 - \frac{2ab}{d}}}. \tag{23}$$

The bipartite unitary operator $V^{(r)}$ is defined by

$$V^{(r)} := \sum_{j \neq r} |j\rangle\langle j| \otimes U_{r,j} + |r\rangle\langle r| \otimes I \tag{24}$$

where the unitary operator $U_{r,j}$ is defined by

$$U_{r,j} = I - |j\rangle\langle j| - |r-1\rangle\langle r-1| + |j\rangle\langle r-1| + |r-1\rangle\langle j|.$$

The bipartite unitary operator $\Delta^{(r)}$ is defined by

$$\Delta^{(r)} := |r\rangle\langle r| \otimes X_d^{-(r-1)} + \sum_{j \neq r} |j\rangle\langle j| \otimes I. \tag{25}$$

The unitary operator $\Gamma^{(r)}$ on $\mathbb{C}^d \otimes \mathbb{C}^d \otimes \mathbb{C}^2$ is defined by

$$\Gamma^{(r)} := |r\rangle\langle r| \otimes \text{swap} + \sum_{j \neq r} |j\rangle\langle j| \otimes I, \tag{26}$$

where swap is a unitary operator on $\mathbb{C}^d \otimes \mathbb{C}^2$ defined by

$$\text{swap} := \sum_{i=2}^{d-1} \sum_{j=0,1} |ij\rangle\langle ij| + \sum_{i,j=0,1} |ij\rangle\langle ji|.$$

The unitary operator Θ on $\mathbb{C}^2 \otimes \mathbb{C}^2$ is defined by

$$\begin{aligned} \Theta|jj\rangle &= |jj\rangle \quad (j = 0, 1) \\ \Theta(\cos \eta|01\rangle + \sin \eta|10\rangle) &= |10\rangle \\ \Theta(\sin \eta|01\rangle - \cos \eta|10\rangle) &= |01\rangle \end{aligned} \tag{27}$$

The bipartite unitary operator $\Lambda^{(r)}$ is defined by

$$\Lambda^{(r)} := \sum_{j \neq r} |j\rangle\langle j| \otimes I + |r\rangle\langle r| \otimes X_d^r \tag{28}$$

Before starting the protocol, we prepare three d -dimensional systems A, B , and M at the source node s , d -dimensional systems C, E , and 2-dimensional systems G, T_1 at the target node t_1 . Similarly, we prepare d -dimensional systems D, F , and 2-dimensional systems H, T_2 at t_2 . The entanglement resource $\cos \eta|0\rangle_E|1\rangle_F + \sin \eta|1\rangle_E|0\rangle_F$ is shared between E and F , and the Bell state $\frac{1}{\sqrt{2}}(|00\rangle_{T_1T_2} + |11\rangle_{T_1T_2})$ is shared between T_1 and T_2 . Thus, the amount of entanglement resources is at most 2 ebits.

The protocol for $1 \rightarrow 2$ is shown as Protocol 2. In Protocol 2, first, asymmetric UQCs of an q^r -dimensional input state $|\psi\rangle$ is created on the source node s at Step 1. Then, by measuring an ancilla, the whole state is splitted into classical information (measurement result), which is sent to target nodes, and a bipartite quantum state at Step 2. The bipartite quantum state is compressed into a q^r -dimensional state at Step 3. The state is distributed to the target nodes t_1 and t_2 by the protocol of Kobayashi et al. at Step 4. From the GHZ-type state received in the previous step and the classical information received at Step 2, target nodes t_1 and t_2 reconstruct asymmetric UQCs of $|\psi\rangle$ by LOCC and preshared small entanglement resource; this process is completed from Step 5 to Step 12. As a result of the protocol, $1 \rightarrow 2$ asymmetric UQCs given by Equation (7) are created in systems EF , where E and F are on the target nodes t_1 and t_2 , respectively. Note that as we explained in the previous subsection, optimal asymmetric UQCs depend on the parameters a and b in Equation (4).

We can set these parameters in Step 2 of the protocol, when we apply $U_{1 \rightarrow 2}^{(a,b)}$. As we already explained,

Protocol 2 1 \rightarrow 2 quantum multicast network coding protocol

- Step 1:** At the beginning, the source node s has an unknown input quantum state $|\psi\rangle_A$ on system A and makes 1 \rightarrow 2 asymmetric universal clones by applying an isometry $U_{1 \rightarrow 2}^{(a,b)}$ defined by Equation (4) from the system A to the system ABM .
- Step 2:** The source node s measures system M in the computational basis and sends the measurement outcome r to the two target nodes t_1 and t_2 .
- Step 3:** The source node s applies the unitary operator Y_{AB} defined by Equations (21) and (22) to the systems AB , then discards the system B .
- Step 4:** The state on system A is multicast to the target nodes t_1 and t_2 over the quantum network G using the protocol of Kobayashi et al. The target nodes t_1 and t_2 put the output GHZ-type state of the protocol of Kobayashi et al. on system CD .
- Step 5:** The target nodes t_1 and t_2 apply $X_d^{r-1} \otimes X_d^{r-1}$ to system EF using the measurement outcome r sent from the source node s .
- Step 6:** The target node t_1 applies $V_{C,E}^{(r)}$ defined by Equation (24) to system CE , and the target node t_2 applies $V_{D,F}^{(r)}$ to system DF . Then, the target node t_1 applies $\Delta_{C,E}^{(r)}$ defined by Equation (25) to system CE , and the target node t_2 applies $\Delta_{D,F}^{(r)}$ to system DF .
- Step 7:** The target node t_1 initializes G in $|0\rangle$ and applies $\Gamma_{C,E,G}^{(r)}$ defined by Equation (26) on system CEG . The target node t_2 initializes H in $|0\rangle$ and applies $\Gamma_{C,E,G}^{(r)}$ to system DFH .
- Step 8:** The target node t_2 sends the state on system H to system T_1 at the target node t_1 using the Bell state on system $T_1 T_2$ by the quantum teleportation.
- Step 9:** The target node t_1 applies Θ_{GT_1} defined by Equation (27) to systems G and T_1 and discards T_1 .
- Step 10:** The target node t_1 measures system G in

$$\left\{ |\tilde{0}\rangle = \frac{|0\rangle + |1\rangle}{\sqrt{2}}, |\tilde{1}\rangle = \frac{|0\rangle - |1\rangle}{\sqrt{2}} \right\}$$

and derives the measurement outcome k . Then, t_1 performs $(I - 2|r\rangle\langle r|)^k$ on system C .

- Step 11:** The target node t_1 applies $\Lambda_{CE}^{(r)}$ defined by Equation (28) on the system CE , and the target node t_2 applies $\Lambda_{DF}^{(r)}$ the system DF .
- Step 12:** The target nodes t_1 and t_2 measure system C and D in the Fourier basis

$$\left\{ \sum_{x=0}^{d-1} \frac{\omega^{px}}{\sqrt{d}} |x\rangle \right\}_{p \in \mathbb{Z}_d},$$

respectively, and derive the measurement outcomes p_1 and p_2 , respectively. Then, t_1 applies $Z_d^{p_1+p_2}$ to system E , and t_2 applies $Z_d^{p_1+p_2}$ to system F .

3.1.2. Proof of 1 \rightarrow 2 Quantum Multicast Protocol

In this sub-subsection, we present the proof that Protocol 2 creates 1 \rightarrow 2 asymmetric UQCs given by Equation (7) in system EF shared by target nodes t_1 and t_2 .

Proof. As we explained in the previous subsection, an input state at the source node s can be written as

$$|\psi\rangle = \sum_{j=0}^{d-1} \alpha_j |j\rangle \in \mathcal{H}_s.$$

Then, from Equation (4), the state on system ABM after step 1 can be written as:

$$a|\psi\rangle_A |\Phi^+\rangle_{BM} + b|\psi\rangle_B |\Phi^+\rangle_{AM} \tag{29}$$

The unnormalized state $|\Psi_2^{(r)}\rangle_{AB}$ on system AB after deriving measurement outcome r in Step 2 can be written as:

$$|\Psi_2^{(r)}\rangle_{AB} := \beta_r |rr\rangle_{AB} + \sum_{j \neq r} \beta_j (\cos \eta |jr\rangle_{AB} + \sin \eta |rj\rangle_{AB}), \tag{30}$$

where η is defined by Equation (23), and $\{\beta_j\}_{j=0}^{d-1}$ is defined by

$$\begin{aligned} \beta_r &= \frac{\alpha_r}{\sqrt{d}}(a + b) \\ \beta_j &= \frac{\alpha_j}{\sqrt{d}} \sqrt{1 - \frac{2ab}{d}} \quad (\forall j \neq r). \end{aligned} \tag{31}$$

here, $\| |\Psi_2^{(r)}\rangle_{AB} \|^2 = \sum_j |\beta_j|^2$ is a probability in which outcome r is derived in Step 2. Since measuring system M without seeing the outcome is mathematically equivalent to tracing out system M , $\{ |\Psi_2^{(r)}\rangle_{r=0}^{d-1} \}$ satisfies

$$\varepsilon_{1 \rightarrow 2}(|\psi\rangle\langle\psi|) = \sum_{r=0}^{d-1} |\Psi_2^{(r)}\rangle\langle\Psi_2^{(r)}|, \tag{32}$$

where $\varepsilon_{1 \rightarrow 2}$ is a $1 \rightarrow 2$ optimal asymmetric UQCM defined by Equation (7). Hence, the purpose of the remaining part of the protocol is to transfer $|\Psi_2^{(r)}\rangle$ to the target nodes. However, in our problem settings, the throughput of the quantum network is too small to send $|\Psi_2^{(r)}\rangle$ directly to the target nodes. Hence, first, we compress the state on the d -dimensional system in Step 3. Then, the unnormalized state of system AB after Step 3 can be written as

$$|\Psi_3\rangle_A = \sum_{j=0}^{d-1} \beta_j |j\rangle_A. \tag{33}$$

In Step 4, the protocol of Kobayashi et al. successfully works based on the assumption for the existence of a classical linear multicast network code. Since the (unnormalized) input state for the protocol of Kobayashi et al. is $|\Psi_3\rangle_A$, the unnormalized state on the system C at the target node t_1 and on system D at the target node t_2 can be written as $\sum_{j=0}^{d-1} \beta_j |j\rangle_C |j\rangle_D$. The purpose of the remaining part of the protocol is to reconstruct $|\Psi_2^{(r)}\rangle$ from this state.

Since system EF is initially on $\cos \eta |0\rangle_E |1\rangle_F + \sin \eta |1\rangle_E |0\rangle_F$, the unnormalized state on system $CDEF$ can be written as

$$\sum_{j=0}^{d-1} \beta_j |jj\rangle_{CD} \otimes (\cos \eta |0\rangle_E |1\rangle_F + \sin \eta |1\rangle_E |0\rangle_F) \tag{34}$$

Then, the unnormalized state on $CDEF$ after Step 5 can be written as

$$\sum_{j=0}^{d-1} \beta_j |jj\rangle_{CD} \otimes (\cos \eta |r-1\rangle_E |r\rangle_F + \sin \eta |r\rangle_E |r-1\rangle_F). \tag{35}$$

The unnormalized state on $CDEF$ after Step 6 is

$$\begin{aligned} &\sum_{j \neq r} \beta_j |jj\rangle_{CD} \otimes (\cos \eta |j\rangle_E |r\rangle_F + \sin \eta |r\rangle_E |j\rangle_F) \\ &+ \beta_r |rr\rangle_{CD} \otimes (\cos \eta |0\rangle_E |1\rangle_F + \sin \eta |1\rangle_E |0\rangle_F). \end{aligned} \tag{36}$$

Then, the unnormalized state on $CDEFGH$ after Step 7 can be written as

$$\sum_{j \neq r} \beta_j |jj\rangle_{CD} \otimes (\cos \eta |j\rangle_E |r\rangle_F + \sin \eta |r\rangle_E |j\rangle_F) \otimes |00\rangle_{GH} + \beta_r |rr\rangle_{CD} \otimes |00\rangle_{EF} \otimes (\cos \eta |0\rangle_G |1\rangle_H + \sin \eta |1\rangle_G |0\rangle_H). \tag{37}$$

Next, in Step 8, the state on the system H is transferred to system T_1 by quantum teleportation [102]. Thus, the unnormalized state on $CDEFG$ after Step 9 can be written as

$$\sum_{j \neq r} \beta_j |jj\rangle_{CD} \otimes (\cos \eta |j\rangle_E |r\rangle_F + \sin \eta |r\rangle_E |j\rangle_F) \otimes |0\rangle_G + \beta_r |rr\rangle_{CD} \otimes |00\rangle_{EF} \otimes |1\rangle_G. \tag{38}$$

Since system G is effectively removed in Step 10, the unnormalized state on system $CDEF$ after Step 10 can be written as

$$\sum_{j \neq r} \beta_j |jj\rangle_{CD} \otimes (\cos \eta |j\rangle_E |r\rangle_F + \sin \eta |r\rangle_E |j\rangle_F) + \beta_r |rr\rangle_{CD} \otimes |00\rangle_{EF}. \tag{39}$$

Then, the unnormalized state on $CDEF$ after Step 11 can be written as

$$\sum_{j \neq r} \beta_j |jj\rangle_{CD} \otimes (\cos \eta |j\rangle_E |r\rangle_F + \sin \eta |r\rangle_E |j\rangle_F) + \beta_r |rr\rangle_{CD} \otimes |rr\rangle_{EF}. \tag{40}$$

In Step 12, after system CD is measured in the Fourier basis $\{d^{-1/2} \cdot \sum_{x=0}^{d-1} \omega^{px} |x\rangle\}_{p \in Z_d}$ and is discarded, the unnormalized state on EF for the measurement outcomes p_1 and p_2 can be written as

$$\sum_{j \neq r} \beta_j \omega^{-j(p_1+p_2)} (\cos \eta |j\rangle_E |r\rangle_F + \sin \eta |r\rangle_E |j\rangle_F) + \beta_r \omega^{-r(p_1+p_2)} |rr\rangle_{EF} \tag{41}$$

Hence, after applying $Z^{p_1+p_2} \otimes Z^{p_1+p_2}$ on system EF , the unnormalized state on EF becomes

$$\omega^{r(p_1+p_2)} \cdot \sum_{j=0, j \neq r}^{d-1} \beta_j (\cos \eta |j\rangle_E |r\rangle_F + \sin \eta |r\rangle_E |j\rangle_F) + \beta_r |rr\rangle_{EF}. \tag{42}$$

This unnormalized state coincides with $|\Psi_2^{(r)}\rangle$ defined by Equation (42) except a global phase. Since Equation (42) is the unnormalized state corresponding to the outcome r in Step 2, the final state of this protocol can be written as $\sum_r |\Psi_2^{(r)}\rangle \langle \Psi_2^{(r)}|$. Hence, by Equation (32), the final states of protocol 2 on the target nodes t_1 and t_2 are $1 \rightarrow 2$ optimal asymmetric UQCs of the input state $|\psi\rangle$. \square

3.2. 1 \rightarrow 3 Optimal Asymmetric Quantum Universal Clones Multicast Protocol

In this subsection, we present a protocol that multicasts optimal asymmetric UQCs from the source node s to three target nodes t_1, t_2 , and t_3 on a quantum network. We present the protocol in Sections 3.2.1 and 3.2.2, we prove that creates optimal asymmetric UQCs.

3.2.1. 1 \rightarrow 3 Quantum Multicast Protocol

In this sub-subsection, we present a protocol that multicasts $1 \rightarrow 3$ optimal asymmetric UQCs of an unknown input quantum state from the source node s to two target nodes t_1, t_2 , and t_3 .

The problem setting for the 1 → 3 quantum multicast protocol is almost the same as that of the 1 → 2 protocol given in the last subsection. Hence, we consider only the difference between these two problem settings. First, the number of target nodes is different. That is, in this subsection, a quantum network G has three target nodes t_1, t_2 , and t_3 . The purpose of the protocol is to construct 1 → 3 optimal asymmetric universal clones given by Equation (12) among target nodes t_1, t_2 , and t_3 for a unknown d -dimensional input state $|\psi\rangle = \sum_{j=0}^d \alpha_j |j\rangle \in \mathcal{H}_s$ on a source node, where \mathcal{H}_s is a d -dimensional input space. We again assume $d = q^r$. In other words, we consider a multicast quantum network code with source rate r . The assumption for the existence of a classical linear multicast network code is also similar. That is, a classical linear multicast network code is a code on \mathbb{F}_q used to multicast from the node s to the nodes t_1, t_2, t_3 on G' with source rate r . The amount of entanglement shared among the target nodes is also different. In 1 → 3 case, we assume that at most $2 + 4 \log_2 3$ ebits are shared among the target nodes t_1, t_2 , and t_3 . Hence, the amount of this entanglement resource is constant with respect to the dimension d of the input state.

Before we present the protocol, we define the unitary operators used in the protocol. In the following definitions, a subscript of an unitary operator denotes the step of the protocol where it is used. Thus, for example, we do not define U_2 since we will not use any unitary operation at Step 2 of the protocol. $U_3^{(r,s)}$ is a tripartite unitary operator satisfying the following conditions:

$$\begin{aligned}
 U_3^{(r,s)} \cdot \frac{\alpha|jrs\rangle + \beta|rjs\rangle + \gamma|rsj\rangle + \alpha|jsr\rangle + \beta|sjr\rangle + \gamma|srj\rangle}{\sqrt{2\alpha^2 + 2\beta^2 + 2\gamma^2}} &= |j00\rangle, \quad (\forall j \neq r, s) \\
 U_3^{(r,s)} \cdot \frac{(\alpha + \beta)|rrs\rangle + (\beta + \gamma)|srr\rangle + (\gamma + \alpha)|rsr\rangle}{\sqrt{(\alpha + \beta)^2 + (\beta + \gamma)^2 + (\gamma + \alpha)^2}} &= |r00\rangle, \\
 U_3^{(r,s)} \cdot \frac{(\alpha + \beta)|ssr\rangle + (\beta + \gamma)|rss\rangle + (\gamma + \alpha)|srs\rangle}{\sqrt{(\alpha + \beta)^2 + (\beta + \gamma)^2 + (\gamma + \alpha)^2}} &= |s00\rangle.
 \end{aligned} \tag{43}$$

$U_5^{(r,s)}$ is a bipartite unitary operator defined by

$$U_5^{(r,s)} := |r\rangle\langle r| \otimes I + |s\rangle\langle s| \otimes I + \sum_{j \neq r,s}^{d-1} |j\rangle\langle j| \otimes \left(\sum_{x=0}^{d-1} |\pi_{jrs}(x)\rangle\langle x| \right), \tag{44}$$

where π_{jrs} is a permutation satisfying the following conditions:

$$\pi_{jrs}(0) = j, \quad \pi_{jrs}(1) = r, \quad \pi_{jrs}(2) = s \tag{45}$$

$U_6^{(r,s)}$ is a tripartite unitary operator defined by

$$U_6^{(r,s)} := |r\rangle\langle r| \otimes swap + |s\rangle\langle s| \otimes swap + \sum_{j \neq r,s}^{d-1} |j\rangle\langle j| \otimes I \otimes I, \tag{46}$$

where $swap$ is a swap operator defined by

$$swap := \sum_{i,j=0}^{d-1} |ij\rangle\langle ji|. \tag{47}$$

$U_7^{(r,s)}$ is a bipartite unitary operator defined by

$$U_7^{(r,s)} := \sum_{i \neq r,s} |i\rangle\langle i| \otimes I + |r\rangle\langle r| \otimes \sum_{j=0}^{d-1} |\pi''_{rs}(j)\rangle\langle j| + |s\rangle\langle s| \otimes \sum_{k=0}^{d-1} |\pi''_{sr}(k)\rangle\langle k|, \tag{48}$$

where π''_{xy} is a permutation satisfying $\pi''_{xy}(0) = x$ and $\pi''_{xy}(1) = y$. U_8 is a unitary operator on $\mathbb{C}^3 \otimes \mathbb{C}^3 \otimes \mathbb{C}^3$ satisfying

$$\begin{aligned} U_8(\alpha''_1|001\rangle + \beta''_1|100\rangle + \gamma''_1|010\rangle) &= |000\rangle \\ U_8(\alpha'_1(|012\rangle + |021\rangle) + \beta'_1(|102\rangle + |201\rangle) + \gamma'_1(|120\rangle + |210\rangle)) &= |100\rangle, \end{aligned} \tag{49}$$

where $\alpha'_1, \beta'_1, \gamma'_1, \alpha''_1, \beta''_1,$ and γ''_1 are defined by

$$\begin{aligned} \alpha'_1 &= \frac{\alpha}{\sqrt{2\alpha^2 + 2\beta^2 + 2\gamma^2}}, \quad \beta'_1 = \frac{\beta}{\sqrt{2\alpha^2 + 2\beta^2 + 2\gamma^2}}, \quad \gamma'_1 = \frac{\gamma}{\sqrt{2\alpha^2 + 2\beta^2 + 2\gamma^2}} \\ \alpha''_1 &= \frac{\alpha + \beta}{\sqrt{(\alpha + \beta)^2 + (\beta + \gamma)^2 + (\gamma + \alpha)^2}}, \quad \beta''_1 = \frac{\beta + \gamma}{\sqrt{(\alpha + \beta)^2 + (\beta + \gamma)^2 + (\gamma + \alpha)^2}}, \\ \gamma''_1 &= \frac{\gamma + \alpha}{\sqrt{(\alpha + \beta)^2 + (\beta + \gamma)^2 + (\gamma + \alpha)^2}}. \end{aligned} \tag{50}$$

$U_9^{(r,s,k)}$ is a unitary operator on \mathbb{C}^d defined by

$$U_9^{(r,s,k)} := \sum_{j \neq r,s} |j\rangle\langle j| + (-1)^k |r\rangle\langle r| + (-1)^k |s\rangle\langle s|. \tag{51}$$

$U_2^{(r)}$ is a tripartite unitary operator satisfying

$$\begin{aligned} U_2^{(r)} \cdot \frac{\alpha|jrr\rangle + \beta|rjr\rangle + \gamma|rrj\rangle}{\sqrt{\alpha^2 + \beta^2 + \gamma^2}} &= |j00\rangle, \quad (\forall j \neq r) \\ U_2^{(r)}|rrr\rangle &= |r00\rangle \end{aligned} \tag{52}$$

$U_5^{(r)}$ is a bipartite unitary operator defined by

$$U_5^{(r)} := |r\rangle\langle r| \otimes I + \sum_{j \neq r} |j\rangle\langle j| \otimes \left(\sum_{x=0}^{d-1} |\pi_{jr}(x)\rangle\langle x| \right), \tag{53}$$

where π_{jr} is a permutation satisfying

$$\pi_{jr}(1) = r, \quad \pi_{jr}(0) = j \tag{54}$$

$U_6^{(r)}$ is a tripartite unitary operator defined by

$$U_6^{(r)} := |r\rangle\langle r| \otimes \text{swap} + \sum_{j \neq r}^{d-1} |j\rangle\langle j| \otimes I \otimes I, \tag{55}$$

where swap is an operator defined by Equation (47). $U_7^{(r)}$ is a tripartite unitary operator defined by

$$U_7^{(r)} := \sum_{i \neq r} |i\rangle\langle i| \otimes I + |r\rangle\langle r| \otimes X_d^r, \tag{56}$$

where X_d is the Pauli X operator defined by Equation (20). U'_8 is a unitary operator on $\mathbb{C}^2 \otimes \mathbb{C}^2 \otimes \mathbb{C}^2$ defined by

$$\begin{aligned} U'_8|000\rangle &= |000\rangle \\ U'_8(\alpha'_2|011\rangle + \beta'_2|101\rangle + \gamma'_2|110\rangle) &= |100\rangle \end{aligned} \tag{57}$$

Finally, $U_9^{(r,k)}$ is a unitary operator on \mathbb{C}^d defined by

$$U_9^{(r,k)} := \sum_{j \neq r} |j\rangle\langle j| + (-1)^k |r\rangle\langle r|. \tag{58}$$

We will also use in the protocol the projective measurement $\{P_k\}_{k=0}^2$ defined by the following equations:

$$P_0 := |\tilde{0}\rangle\langle\tilde{0}|, P_1 := |\tilde{1}\rangle\langle\tilde{1}|, P_2 := I - |\tilde{0}\rangle\langle\tilde{0}| - |\tilde{1}\rangle\langle\tilde{1}|, \tag{59}$$

where $|\tilde{0}\rangle := \frac{|0\rangle+|1\rangle}{\sqrt{2}}, |\tilde{1}\rangle := \frac{|0\rangle-|1\rangle}{\sqrt{2}}$.

At the beginning of the protocol, the source node s has five d -dimensional systems $A, B, C, R,$ and S . The target node t_1 has three d -dimensional systems $D, M_1,$ and N_1 . The target node t_2 has three d -dimensional systems $E, M_2,$ and N_2 . The target node t_3 has three d -dimensional systems $F, M_3,$ and N_3 . Furthermore, the target nodes t_1 and t_2 share $1 + 2 \log_2 3$ ebits of entanglement, and the target nodes t_1 and t_2 share $1 + 2 \log_2 3$ ebits of entanglement in the form of maximally entangled states. Hence, the amount of entanglement resources are $2 + 4 \log_2 3$ ebits in total.

The beginning of the protocol for $1 \rightarrow 3$ is given in Protocol 3. In Protocol 3, first, asymmetric UQCs of an q^r -dimensional input state $|\psi\rangle$ is created on the source node s at Step 1. Then, by measuring ancillary systems R and S , the whole state is splitted into classical information (measurement results r and s), which is sent to target nodes and a tripartite quantum state at Step 2. The continuation of the protocol branches depending on whether $r \neq s$ or $r = s$. The continuation for $r \neq s$ is given in Protocol 4, and for $r = s$ is given in Protocol 5. In both Protocols 4 and 5, the tripartite quantum state is compressed into a q^r -dimensional state at Step 3. The state is distributed to the target nodes $t_1, t_2,$ and t_3 by the protocol of Kobayashi et al. at Step 4. From the GHZ-type state received in the previous step and the classical information received at Step 2, target nodes $t_1, t_2,$ and t_3 reconstruct asymmetric UQCs of $|\psi\rangle$ by LOCC and preshared small entanglement resource; this process is completed in the remaining part of the protocols. As the result of the protocol, $1 \rightarrow 3$ asymmetric UQCs given by Equation (12) are created system $M_1M_2M_3$, where $M_1, M_2,$ and M_3 are on the target nodes $t_1, t_2,$ and t_3 , respectively. Note that as we explained in the previous subsection, asymmetric UQCs depends on the parameters $\alpha, \beta,$ and γ in Equation (10). We can set these parameters in step 1 of the protocol, when we apply $U_{1 \rightarrow 3}^{(\alpha,\beta,\gamma)}$.

Protocol 3 $1 \rightarrow 3$ quantum multicast network coding protocol (beginning)

Step 1: At the beginning, the source node s has an unknown input quantum state $|\psi\rangle_A$ on system A , and makes $1 \rightarrow 3$ asymmetric universal clones by applying an isometry

$U_{1 \rightarrow 3}^{(\alpha,\beta,\gamma)}$ defined by Equation (10) from system A to system $ABCRS$.

Step 2: The source node s measures the systems R and S in the computational basis, where the measurement outcomes of R and S are called r and s , respectively. The source node s sends the measurement outcomes r and s to the target nodes $t_1, t_2,$ and t_3 . The following steps of the protocol depend on whether $r \neq s$ or $r = s$.

Protocol 4 Continuation of Protocol 3 for 1 → 3 quantum multicast network coding (for $r \neq s$)

[$r \neq s$]

Step 3: The source node s applies unitary operator $U_2^{(r,s)}$ defined by Equation (43) to system ABC , and then, discards systems B and C .

Step 4: The state on system A is multicast to the target nodes t_1, t_2 , and t_3 over the quantum network G using the protocol of Kobayashi et al. The target nodes t_1, t_2 , and t_3 put the output of the protocol of Kobayashi et al. on system DEF . Then, using $2 \log_2 3$ ebits of entanglement, the targets nodes share the following state on system $M_1M_2M_3$:

$$(\alpha'_1(|012\rangle + |021\rangle) + \beta'_1(|102\rangle + |201\rangle) + \gamma'_1(|120\rangle + |210\rangle))_{M_1, M_2, M_3},$$

where α'_1, β'_1 , and γ'_1 are defined by Equation (50). Furthermore, by using 2 ebits of entanglement, the target nodes share the following state on system $N_1N_2N_3$:

$$(\alpha''_1|001\rangle + \beta''_1|100\rangle + \gamma''_1|010\rangle)_{N_1, N_2, N_3}, \tag{60}$$

where α''_1, β''_1 and γ''_1 are defined by Equation (50).

Step 5: The target nodes apply $U_{5,DM_1}^{(r,s)} \otimes U_{5,EM_2}^{(r,s)} \otimes U_{5,FM_3}^{(r,s)}$ to system $DM_1EM_2FM_3$, where $U_5^{(r,s)}$ is defined by Equation (44).

Step 6: The target nodes apply $U_{6,DM_1N_1}^{(r,s)} \otimes U_{6,EM_2N_2}^{(r,s)} \otimes U_{6,FM_3N_3}^{(r,s)}$ to system $DM_1N_1EM_2N_2FM_3N_3$, where $U_6^{(r,s)}$ is defined by Equation (46).

Step 7: The target nodes apply $U_{7,DM_1}^{(r,s)} \otimes U_{7,EM_2}^{(r,s)} \otimes U_{7,FM_3}^{(r,s)}$ to system $DM_1EM_2FM_3$, where $U_7^{(r,s)}$ is defined by Equation (48).

Step 8: Using $2 \log_2 3$ ebits of entanglement resource, subspaces spanned by $\{|0\rangle, |1\rangle, |2\rangle\}$ of the systems N_2 and N_3 are sent from the target nodes t_2 and t_3 to the target node t_1 , respectively. The target node t_1 applies $U_{8,N_1N_2N_3}$ to system $N_1N_2N_3$ and discards systems N_2 and N_3 .

Step 9: The target node t_1 applies the projective measurement $\{P_k\}_{k=0}^2$ defined by Equation (59) on system N_1 in the basis and discards the quantum system N_1 . Then, depending on the measurement outcome k , the target node t_1 applies $U_9^{(r,s,k)}$ defined by Equation (51) on system D .

Step 10: The target nodes t_1, t_2 , and t_3 measure system D, E , and F in the Fourier basis $\{d^{-1/2} \cdot \sum_{x=0}^{d-1} \omega^{px} |x\rangle\}_{p \in \mathbb{Z}_d}$, respectively. Then, they apply $Z^{(p_1+p_2+p_3)} \otimes Z^{(p_1+p_2+p_3)} \otimes Z^{(p_1+p_2+p_3)}$ to system $M_1M_2M_3$, where p_1, p_2 , and p_3 are the measurement outcomes on the target nodes t_1, t_2 , and t_3 , respectively.

Protocol 5 Continuation of Protocol 3 for 1 → 3 quantum multicast network coding (for $r = s$)

[$r = s$]

Step 3: The source node s applies unitary operator $U_3^{(r)}$ defined by Equation (52) to system ABC and then discards the systems B and C .

Step 4: The state on system A is multicast to the target nodes $t_1, t_2,$ and t_3 over the quantum network G using the protocol of Kobayashi et al. The target nodes $t_1, t_2,$ and t_3 put the output of the protocol of Kobayashi et al. on system DEF . Then, using 2 ebits of entanglement, the target nodes share the following state on system $M_1M_2M_3$:

$$(\alpha'_2|011\rangle + \beta'_2|101\rangle + \gamma'_2|110\rangle)_{M_1M_2M_3'} \tag{61}$$

where $\alpha'_2 = \frac{2\alpha}{\sqrt{(2\alpha)^2+(2\beta)^2+(2\gamma)^2}}, \beta'_2 = \frac{2\beta}{\sqrt{(2\alpha)^2+(2\beta)^2+(2\gamma)^2}}$ and $\gamma'_2 = \frac{2\gamma}{\sqrt{(2\alpha)^2+(2\beta)^2+(2\gamma)^2}}$.

Furthermore, they initialize all the systems $N_1, N_2,$ and N_3 in $|0\rangle$.

Step 5: The target nodes apply $U_{5,DM_1}^{(r)} \otimes U_{5,EM_2}^{(r)} \otimes U_{5,FM_3}^{(r)}$ to system $DM_1EM_2FM_3$, where $U_5^{(r)}$ is defined by Equation (53).

Step 6: The target nodes apply $U_{6,DM_1N_1}^{(r)} \otimes U_{6,EM_2N_2}^{(r)} \otimes U_{6,FM_3N_3}^{(r)}$ to system $DM_1N_1EM_2N_2FM_3N_3$, where $U_6^{(r)}$ is defined by Equation (55).

Step 7: The target nodes apply $U_{7,DM_1}^{(r)} \otimes U_{7,EM_2}^{(r)} \otimes U_{7,FM_3}^{(r)}$ to system $DM_1EM_2FM_3$, where $U_7^{(r)}$ is defined by Equation (56).

Step 8: By using 2 ebits of entanglement resource, subspaces spanned by $\{|0\rangle, |1\rangle\}$ of the systems N_2 and N_3 are sent from the target nodes t_2 and t_3 to the target node t_1 , respectively. The target node t_1 applies $U_{8,N_1N_2N_3}^{(r)}$ as defined by Equation (57) to system $N_1N_2N_3$ and discards system N_2 and N_3 .

Step 9: The target node t_1 applies the projective measurement $\{P_k\}_{k=0}^2$ defined by Equation (59) on system N_1 in the basis and discards the quantum system N_1 . Then, depending on the measurement outcome k , the target node t_1 applies $U_9^{(r,k)}$ defined by Equation (58) on the system D .

Step 10: The target nodes $t_1, t_2,$ and t_3 measure system $D, E,$ and F in the Fourier basis $\{d^{-1/2} \cdot \sum_{x=0}^{d-1} \omega^{px}|x\rangle\}_{p \in \mathbb{Z}_d}$, respectively. Then, they apply $Z_d^{(p_1+p_2+p_3)} \otimes Z_d^{(p_1+p_2+p_3)} \otimes Z_d^{(p_1+p_2+p_3)}$ to system $M_1M_2M_3$, where $p_1, p_2,$ and p_3 are the measurement outcomes on the target nodes $t_1, t_2,$ and t_3 , respectively.

3.2.2. Proof of 1 → 3 Quantum Multicast Protocol

In this sub-subsection, we prove that Protocols 3–5 create 1 → 3 asymmetric UQCs given by Equation (12) in system $M_1M_2M_3$.

Proof. Let the input state at the source node be $|\psi\rangle = \sum_{j=0}^{d-1} \delta_j|j\rangle$. Then, from Equation (10), the state on system $ABCRS$ after Step 1 can be written as

$$\begin{aligned} &\sqrt{\frac{d}{2d+2}}[\alpha|\psi\rangle_A(|\Phi^+\rangle_{BR}|\Phi^+\rangle_{CS} + |\Phi^+\rangle_{BS}|\Phi^+\rangle_{CR}) \\ &\quad + \beta|\psi\rangle_B(|\Phi^+\rangle_{AR}|\Phi^+\rangle_{CS} + |\Phi^+\rangle_{AS}|\Phi^+\rangle_{CR}) \\ &\quad + \gamma|\psi\rangle_C(|\Phi^+\rangle_{AR}|\Phi^+\rangle_{BS} + |\Phi^+\rangle_{AS}|\Phi^+\rangle_{BR})] \end{aligned} \tag{62}$$

After Step 2, the protocol branches depending on whether $r \neq s$ or $r = s$, where r and s are the measurement outcomes of system R and S , respectively.

The unnormalized state $|\Psi_2^{(r,s)}\rangle$ after Step 2 for $r \neq s$ can be written as

$$\begin{aligned} & |\Psi_2^{(r,s)}\rangle \\ &= \frac{1}{\sqrt{2d(d+1)}} \left[\alpha(|\psi\rangle_A|r\rangle_B|s\rangle_C + |\psi\rangle_A|s\rangle_B|r\rangle_C) + \beta(|r\rangle_A|\psi\rangle_B|s\rangle_C + |s\rangle_A|\psi\rangle_B|r\rangle_C) \right. \\ &\quad \left. + \gamma(|r\rangle_A|s\rangle_B|\psi\rangle_C + |s\rangle_A|r\rangle_B|\psi\rangle_C) \right] \\ &= \frac{1}{\sqrt{2d(d+1)}} \left[\delta_r((\alpha + \beta)|rrs) + (\beta + \gamma)|srr) + (\gamma + \alpha)|rsr) \right]_{ABC} \\ &\quad + \delta_s((\alpha + \beta)|ssr) + (\beta + \gamma)|rss) + (\gamma + \alpha)|srs) \Big]_{ABC} \\ &\quad + \sum_{j \neq r,s} \delta_j(\alpha|jrs) + \beta|rjs) + \gamma|rsj) + \alpha|jsr) + \beta|sjr) + \gamma|srj) \Big]_{ABC}. \end{aligned} \tag{63}$$

The unnormalized state $|\Psi_2^{(r,r)}\rangle$ after Step 2 for $r = s$ can be written

$$\begin{aligned} & |\Psi_2^{(r,r)}\rangle \\ &= \sqrt{\frac{2}{d(d+1)}} \left[\alpha|\psi\rangle_A|r\rangle_B|r\rangle_C + \beta|r\rangle_A|\psi\rangle_B|r\rangle_C + \gamma|r\rangle_A|r\rangle_B|\psi\rangle_C \right] \\ &= \sqrt{\frac{2}{d(d+1)}} \left[\delta_r(\alpha + \beta + \gamma)|rrr) + \sum_{j \neq r} \delta_j(\alpha|jrr) + \beta|rjr) + \gamma|rrj) \right]. \end{aligned} \tag{64}$$

As for the $1 \rightarrow 2$ quantum multicast network coding protocol, $\{|\Psi_2^{(r,s)}\rangle\}_{r,s=0}^{d-1}$ satisfies

$$\epsilon_{1 \rightarrow 3}^{\alpha,\beta,\gamma}(|\psi\rangle\langle\psi|) = \sum_{r,s=0}^{d-1} |\Psi_2^{(r,s)}\rangle\langle\Psi_2^{(r,s)}|, \tag{65}$$

where $\epsilon_{1 \rightarrow 3}^{\alpha,\beta,\gamma}$ is a $1 \rightarrow 3$ optimal asymmetric UQCM defined by Equation (12). Hence, the purpose of the remaining part of the protocol is to transfer $|\Psi_2^{(r,s)}\rangle$ to the target nodes.

First, we give the continuation of the proof for $r \neq s$ (Protocol 4). We compress the state on a d -dimensional system on step 3. The unnormalized state on system A after Step 3 can be written as

$$\sum_{j=0}^{d-1} \kappa_j |j\rangle, \tag{66}$$

where $\{\kappa_j\}_{j=0}^{d-1}$ is defined as

$$\begin{aligned} \kappa_j &= \sqrt{\frac{d}{2d+2}} \frac{\delta_j}{d} \sqrt{2\alpha^2 + 2\beta^2 + 2\gamma^2} \quad (j \neq r, s), \\ \kappa_r &= \sqrt{\frac{d}{2d+2}} \frac{\delta_r}{d} \sqrt{(\alpha + \beta)^2 + (\beta + \gamma)^2 + (\gamma + \alpha)^2}, \\ \kappa_s &= \sqrt{\frac{d}{2d+2}} \frac{\delta_s}{d} \sqrt{(\alpha + \beta)^2 + (\beta + \gamma)^2 + (\gamma + \alpha)^2}. \end{aligned} \tag{67}$$

In Step 4, the protocol of Kobayashi et al. successfully works based on the assumption for the existence of a classical linear multicast network code. The unnormalized state on systems DEF shared by the target nodes $t_1, t_2,$ and t_3 can be written as

$$\sum_{j=0}^{d-1} \kappa_j |j\rangle_D |j\rangle_E |j\rangle_F.$$

Hence, the unnormalized state after Step 4 can be written as

$$\begin{aligned} & \sum_{j=0}^{d-1} \kappa_j |jjj\rangle_{DEF} \otimes \left(\alpha'_1 |012\rangle + \beta'_1 |102\rangle + \gamma'_1 |120\rangle + \alpha'_1 |021\rangle + \beta'_1 |201\rangle + \gamma'_1 |210\rangle \right)_{M_1 M_2 M_3} \\ & \otimes (\alpha''_1 |001\rangle + \beta''_1 |100\rangle + \gamma''_1 |010\rangle)_{N_1 N_2 N_3} \end{aligned} \tag{68}$$

The purpose of the remaining part of the protocol is to reconstruct $|\Psi_2^{(r,s)}\rangle$ from the above state. The unnormalized state after Step 5 can be written as

$$\begin{aligned} & \left(\sum_{j \neq r,s}^{d-1} \kappa_j |jjj\rangle_{DEF} \otimes (\alpha'_1 |jrs\rangle + \beta'_1 |rjs\rangle + \gamma'_1 |rsj\rangle + \alpha'_1 |jsr\rangle + \beta'_1 |sjr\rangle + \gamma'_1 |srj\rangle)_{M_1 M_2 M_3} \right. \\ & + (\kappa_r |rrr\rangle_{DEF} + \kappa_s |sss\rangle_{DEF}) \\ & \left. \otimes (\alpha'_1 |012\rangle + \beta'_1 |102\rangle + \gamma'_1 |120\rangle + \alpha'_1 |021\rangle + \beta'_1 |201\rangle + \gamma'_1 |210\rangle)_{M_1 M_2 M_3} \right) \\ & \otimes (\alpha''_1 |001\rangle + \beta''_1 |100\rangle + \gamma''_1 |010\rangle)_{N_1 N_2 N_3} \end{aligned} \tag{69}$$

The unnormalized state after Step 6 can be written as

$$\begin{aligned} & \sum_{j \neq r,s}^{d-1} \kappa_j |jjj\rangle_{DEF} \otimes (\alpha'_1 |jrs\rangle + \beta'_1 |rjs\rangle + \gamma'_1 |rsj\rangle + \alpha'_1 |jsr\rangle + \beta'_1 |sjr\rangle + \gamma'_1 |srj\rangle)_{M_1 M_2 M_3} \\ & \otimes (\alpha''_1 |001\rangle + \beta''_1 |100\rangle + \gamma''_1 |010\rangle)_{N_1 N_2 N_3} \\ & + (\kappa_r |rrr\rangle + \kappa_s |sss\rangle)_{DEF} \otimes (\alpha''_1 |001\rangle + \beta''_1 |100\rangle + \gamma''_1 |010\rangle)_{M_1 M_2 M_3} \\ & \otimes (\alpha'_1 |012\rangle + \beta'_1 |102\rangle + \gamma'_1 |120\rangle + \alpha'_1 |021\rangle + \beta'_1 |201\rangle + \gamma'_1 |210\rangle)_{N_1 N_2 N_3} \end{aligned} \tag{70}$$

Then, the unnormalized state after Step 7 can be written as

$$\begin{aligned} & \sum_{j \neq r,s}^{d-1} \kappa_j |jjj\rangle_{DEF} \otimes (\alpha'_1 |jrs\rangle + \beta'_1 |rjs\rangle + \gamma'_1 |rsj\rangle + \alpha'_1 |jsr\rangle + \beta'_1 |sjr\rangle + \gamma'_1 |srj\rangle)_{M_1 M_2 M_3} \\ & \otimes (\alpha''_1 |001\rangle + \beta''_1 |100\rangle + \gamma''_1 |010\rangle)_{N_1 N_2 N_3} \\ & + \kappa_r |rrr\rangle_{DEF} \otimes (\alpha''_1 |rrs\rangle + \beta''_1 |srr\rangle + \gamma''_1 |rsr\rangle)_{M_1 M_2 M_3} \\ & \otimes (\alpha'_1 |012\rangle + \beta'_1 |102\rangle + \gamma'_1 |120\rangle + \alpha'_1 |021\rangle + \beta'_1 |201\rangle + \gamma'_1 |210\rangle)_{N_1 N_2 N_3} \\ & + \kappa_s |sss\rangle_{DEF} \otimes (\alpha''_1 |ssr\rangle + \beta''_1 |rss\rangle + \gamma''_1 |srs\rangle)_{M_1 M_2 M_3} \\ & \otimes (\alpha'_1 |012\rangle + \beta'_1 |102\rangle + \gamma'_1 |120\rangle + \alpha'_1 |021\rangle + \beta'_1 |201\rangle + \gamma'_1 |210\rangle)_{N_1 N_2 N_3} \end{aligned} \tag{71}$$

The unnormalized state after Step 8 can be written as

$$\begin{aligned} & \sum_{j \neq r,s}^{d-1} \kappa_j |jjj\rangle_{DEF} \otimes (\alpha'_1 |jrs\rangle + \beta'_1 |rjs\rangle + \gamma'_1 |rsj\rangle + \alpha'_1 |jsr\rangle + \beta'_1 |sjr\rangle + \gamma'_1 |srj\rangle)_{M_1 M_2 M_3} \otimes |0\rangle_{N_1} \\ & + \kappa_r |rrr\rangle_{DEF} \otimes (\alpha''_1 |rrs\rangle + \beta''_1 |srr\rangle + \gamma''_1 |rsr\rangle)_{M_1 M_2 M_3} \otimes |1\rangle_{N_1} \\ & + \kappa_s |sss\rangle_{DEF} \otimes (\alpha''_1 |ssr\rangle + \beta''_1 |rss\rangle + \gamma''_1 |srs\rangle)_{M_1 M_2 M_3} \otimes |1\rangle_{N_1} \end{aligned} \tag{72}$$

The unnormalized state after Step 9 can be written as

$$\begin{aligned} & \sum_{j \neq r,s}^{d-1} \kappa_j |jjj\rangle_{DEF} \otimes (\alpha'_1 |jrs\rangle + \beta'_1 |rjs\rangle + \gamma'_1 |rsj\rangle + \alpha'_1 |jsr\rangle + \beta'_1 |sjr\rangle + \gamma'_1 |srj\rangle)_{M_1 M_2 M_3} \\ & + \kappa_r |rrr\rangle_{DEF} \otimes (\alpha''_1 |rrs\rangle + \beta''_1 |srr\rangle + \gamma''_1 |rsr\rangle)_{M_1 M_2 M_3} \\ & + \kappa_s |sss\rangle_{DEF} \otimes (\alpha''_1 |ssr\rangle + \beta''_1 |rss\rangle + \gamma''_1 |srs\rangle)_{M_1 M_2 M_3} \end{aligned} \tag{73}$$

The unnormalized state after Step 10 can be written as

$$\begin{aligned} \omega^{(p_1+p_2+p_3)(r+s)} & \left\{ \sum_{j \neq r,s}^{d-1} \kappa_j (\alpha'_1 |jrs\rangle + \beta'_1 |rjs\rangle + \gamma'_1 |rsj\rangle + \alpha'_1 |jsr\rangle + \beta'_1 |sjr\rangle + \gamma'_1 |srj\rangle)_{M_1 M_2 M_3} \right. \\ & + \kappa_r (\alpha''_1 |rrs\rangle + \beta''_1 |srr\rangle + \gamma''_1 |rsr\rangle)_{M_1 M_2 M_3} \\ & \left. + \kappa_s (\alpha''_1 |ssr\rangle + \beta''_1 |rss\rangle + \gamma''_1 |srs\rangle)_{M_1 M_2 M_3} \right\} \end{aligned} \tag{74}$$

We can easily see that the above state is equivalent to $|\Psi_2^{(r,s)}\rangle$ as defined by Equation (63) except for a global phase. Hence, the proof is complete for $r \neq s$.

Next, we give the continuation of the proof for $r = s$ (Protocol 5). Equation (64) guarantees that the unnormalized state on system A after Step 3 can be written as

$$\sum_{j=0}^{d-1} \kappa'_j |j\rangle, \tag{75}$$

where $\{\kappa_j\}_{j=0}^{d-1}$ is defined as

$$\kappa'_j = \sqrt{\frac{2}{d(d+1)}} \delta_j \sqrt{\alpha^2 + \beta^2 + \gamma^2} \quad (j \neq r), \quad \kappa'_r = \sqrt{\frac{2}{d(d+1)}} \delta_r (\alpha + \beta + \gamma). \tag{76}$$

In Step 4, the protocol of Kobayashi et al. successfully works, and the unnormalized state at the target nodes can be written as $\sum_{j=0}^{d-1} \kappa_j |j\rangle_D |j\rangle_E |j\rangle_F$. Hence, the unnormalized state after Step 4 can be written as

$$\sum_{j=0}^{d-1} \kappa'_j |jjj\rangle_{DEF} \otimes (\alpha'_2 |011\rangle + \beta'_2 |101\rangle + \gamma'_2 |110\rangle)_{M_1 M_2 M_3} \otimes |000\rangle_{N_1 N_2 N_3} \tag{77}$$

Then, the unnormalized state after Step 5 can be written as

$$\begin{aligned} & \sum_{j \neq r}^{d-1} \kappa'_j |jjj\rangle_{DEF} \otimes (\alpha'_2 |jrr\rangle + \beta'_2 |rjr\rangle + \gamma'_2 |rrj\rangle)_{M_1 M_2 M_3} \otimes |000\rangle_{N_1 N_2 N_3} \\ & + \kappa'_r |rrr\rangle_{DEF} \otimes (\alpha'_2 |011\rangle + \beta'_2 |101\rangle + \gamma'_2 |110\rangle)_{M_1 M_2 M_3} \otimes |000\rangle_{N_1 N_2 N_3} \end{aligned} \tag{78}$$

The unnormalized state after Step 6 can be written as

$$\begin{aligned} & \sum_{j \neq r}^{d-1} \kappa'_j |jjj\rangle_{DEF} \otimes (\alpha'_2 |jrr\rangle + \beta'_2 |rjr\rangle + \gamma'_2 |rrj\rangle)_{M_1 M_2 M_3} \otimes |000\rangle_{N_1 N_2 N_3} \\ & + \kappa'_r |rrr\rangle_{DEF} \otimes |000\rangle_{M_1 M_2 M_3} (\alpha'_2 |011\rangle + \beta'_2 |101\rangle + \gamma'_2 |110\rangle)_{N_1 N_2 N_3} \end{aligned} \tag{79}$$

The unnormalized state after Step 7 can be written as

$$\sum_{j \neq r}^{d-1} \kappa'_j |jjj\rangle_{DEF} \otimes (\alpha'_2 |jrr\rangle + \beta'_2 |rjr\rangle + \gamma'_2 |rrj\rangle)_{M_1 M_2 M_3} \otimes |000\rangle_{N_1 N_2 N_3} + \kappa'_r |rrr\rangle_{DEF} \otimes |rrr\rangle_{M_1 M_2 M_3} (\alpha'_2 |011\rangle + \beta'_2 |101\rangle + \gamma'_2 |110\rangle)_{N_1 N_2 N_3} \tag{80}$$

Then, the unnormalized state after Step 8 can be written as

$$\sum_{j \neq r}^{d-1} \kappa'_j |jjj\rangle_{DEF} \otimes (\alpha'_2 |jrr\rangle + \beta'_2 |rjr\rangle + \gamma'_2 |rrj\rangle)_{M_1 M_2 M_3} \otimes |0\rangle_{N_1} + \kappa'_r |rrr\rangle_{DEF} \otimes |rrr\rangle_{M_1 M_2 M_3} |1\rangle_{N_1} \tag{81}$$

The unnormalized state after Step 9 can be written as

$$\sum_{j \neq r}^{d-1} \kappa'_j |jjj\rangle_{DEF} \otimes (\alpha'_2 |jrr\rangle + \beta'_2 |rjr\rangle + \gamma'_2 |rrj\rangle)_{M_1 M_2 M_3} + \kappa'_r |rrr\rangle_{DEF} \otimes |rrr\rangle_{M_1 M_2 M_3} \tag{82}$$

Finally, the unnormalized state after Step 10 can be written as

$$\omega^{(p'_1+p'_2+p'_3)2r} \left\{ \sum_{j=0, j \neq r}^{d-1} \kappa'_j (\alpha'_2 |jrr\rangle + \beta'_2 |rjr\rangle + \gamma'_2 |rrj\rangle)_{M_1 M_2 M_3} + \kappa'_r |rrr\rangle_{M_1 M_2 M_3} \right\} \tag{83}$$

We can easily see that the above state is equivalent to $|\Psi_2^{(r,r)}\rangle$ as defined by Equation (64) except for a global phase. Hence, the proof is complete for $r = s$. Thus, we have achieved multicasting of asymmetric optimal clones for the systems $M_1, M_2,$ and M_3 to the three target nodes. \square

4. Discussion

In this section, we discuss the results derived in the previous section. We give a discussion about the comparison with a conventional scheme in the Section 4.1, the relationship with our protocol and quantum telecloning in Section 4.2, the possibility of the extension of the results in the subsection Section 4.3, and a summary of the results in the Section 4.4.

4.1. Comparison with a Conventional Schemes

In this subsection, we compare our protocol with a conventional protocol without network coding based on entanglement swapping (or quantum repeater [25,26,28,32]), where maximally entangled states are distilled between a source node and a target node; then, asymmetric optimal UQCs are sent by teleportation. For simplicity, we concentrate on the multicast butterfly network, which is given as an undirected underlying graph of the directed graph on the left-hand side of Figure 1. Suppose each channel on the quantum network can transmit a q -dimensional quantum system in a single session, where q is a prime power, and the target nodes share 2 ebit of entanglement. Then, since the rate of the linear solvable network code given on the left-hand side of Figure 1 is 2, our protocol can multicast an asymmetric optimal UQC of a q^2 -dimensional unknown input state from source node s to target nodes t_0 and t_1 .

When we do not use the network coding scheme, a conventional scheme may be given as follows: First, maximally entangled states are distilled between source node s and target nodes t_0 and t_1 . Then, quantum teleportation is implemented to send an asymmetric optimal UQC from source node s to target nodes t_0 and t_1 . Since there are only two channels connected to the source node, there is no way to share more than $2 \log_2 q$ ebit between the source node and the other nodes of the networks [25,26,28].

Hence, the best strategy in the first step is that $\log_2 q$ ebit is shared between the source node share and target node t_0 , and other $\log_2 q$ ebit is also shared between the source node share and target node t_1 . Thus, the source node can only teleport an asymmetric optimal UQC of a q -dimensional unknown input state to the target nodes. Therefore, the rate of the conventional scheme is just a half of our scheme. We note that 2 ebit of entanglement shared between the target nodes is not used in this conventional scheme.

4.2. Relation to Quantum Telecloning

In this subsection, we discuss the relationship with our protocol and quantum telecloning [99,100,103–105]. We first give a short review of quantum telecloning. Quantum telecloning is a protocol to multicast an optimal UQC from a sender to multiple receivers by local operation and classical communication with help of a preshared entangled state. There are various different variations of telecloning protocols [99,100,103–105]. Among them, the one that is strongly related to our problem is Ghiu’s protocol to multicast $1 \rightarrow 2$ asymmetric optimal UQCs [99]. In Ghiu’s protocol, the state $|Y\rangle_{RABM}$ defined by

$$|Y\rangle_{RABM} := I_R \otimes U_{1 \rightarrow 2}^{(a,b)} |\Phi_d^+\rangle_{RA'} \tag{84}$$

is shared among a sender and the first and second receivers, where $U_{1 \rightarrow 2}^{(a,b)}$ is defined by Equation (4) and $|\Phi_d^+\rangle$ is a standard maximally entangled state. The sender, the first receiver, and the second receiver possess the system R , A , and B , respectively. The system M can be possessed by anyone since we do not need to apply any operation on M . The sender further possesses an unknown state $|\psi\rangle$ on the additional system S . At the first step of Ghiu’s protocol, the sender applies a generalized Bell measurement on RS , and sends the measurement outcome to the receivers. Then, the resulted state on ABM is an asymmetric optimal UQCs given by Equation (4) with an error depending on the measurement outcomes. Ghiu proved that there exist local unitary operations on ABM that corrects this error [99]. As a result of the local unitary operations, the asymmetric optimal UQCs are shared between the target nodes. Note that since M is just an ancillary system, we do not necessarily correct the error.

If we consider a way to use Ghiu’s protocol for our problem on the multicast butterfly network, the problem reduces to finding an efficient way to share $|Y\rangle_{RABM}$ among the source node and the two target nodes. A conventional strategy to share this state may be as follows: First, maximally entangled states are shared among the source node and target nodes by using quantum channels on the network. Second, $|Y\rangle_{RABM}$ is prepared on the source node. Finally, the system A and B are teleported to the target nodes by using the maximally entangled states. However, this protocol is almost the same as the conventional protocol presented in the previous subsection, which is the protocol just teleporting asymmetric optimal QCMs using shared maximally entangled states. Thus, the rate of this protocol is also half of the rate of our protocol using network coding.

We can easily see that the system M does not need to be used on Ghiu’s protocol, and his telecloning protocol works just using the state ρ_{RAB} defined by

$$\rho_{RAB} := \text{Tr}_M |Y\rangle\langle Y|_{RABM}. \tag{85}$$

Our protocol can be used to share the state ρ_{RAB} among the source node and the two target nodes as follows. Suppose that there is a quantum network satisfying the assumption used in our $1 \rightarrow 2$ protocol. That is, it has a source node and two target nodes, the target nodes share 2 ebit, and the corresponding classical network has a classical solvable linear network code with rate r . Suppose each quantum channel on the quantum network can transmit q -dimensional system in a single session. Then, first, the source node prepares $|\Phi_{q^r}^+\rangle$ on the system RA . Second, the source node applies our protocol using the system A as an input system. Then, we can easily see that as a result of our protocol, ρ_{RAB} defined by Equation (85) is shared among the source node and the two target nodes. Here, we

emphasize that the dimension of R (as well as A and B) is q^r . That is, the rate of this protocol is again r . For example, in the case of the multicast butterfly network, the rate is 2, which is double the conventional scheme that is explained above. Hence, our protocol can be used as an efficient preparation for asymmetric telecloning over quantum networks.

4.3. Possibility of the Extension of Our Protocol for More than 3 Receivers

In this subsection, we consider a possible extension of our protocol for more than 3 receivers. As a result, we suggest that there might not exist a straightforward extension of the protocol for an arbitrary number of terminal nodes using existing asymmetric optimal UQC schemes. In other words, we estimate that if we use an existing scheme, in order to multicast a d -dimensional unknown state, target nodes need to share $O(\log d)$ ebit of entanglement.

At first, we note that there are not so many existing works about asymmetric optimal UQCs outputting more than 3 copies. That is, Ren et al. and Ćwikliński et al. studied $1 \rightarrow 4$ asymmetric optimal UQCs [82,83], and Key et al. studied $1 \rightarrow N$ asymmetric optimal UQCs [81,84]. Since only existing $1 \rightarrow N$ asymmetric optimal UQC scheme is one given by Key et al., we focus on applying their scheme for multicast communication on quantum networks in this subsection.

Suppose \mathcal{H}_I and \mathcal{H}_O are a d -dimensional input space and a d^N dimensional output space, respectively, and N satisfies $N \geq 3$. Then, the $1 \rightarrow N$ asymmetric optimal UQC of Key et al. [84] is given by the following isometry $U_{I \rightarrow O}$ from \mathcal{H}_I to \mathcal{H}_O :

$$U_{I \rightarrow O} := \sum_{i,j=0}^{d-1} \beta_1 |ji \cdots ii\rangle \langle j| + \beta_2 |ij \cdots ii\rangle \langle j| + \cdots + \beta_N |ii \cdots ij\rangle \langle j|, \tag{86}$$

where $\{\beta_n\}_{n=1}^N$ is an eigenvector corresponding to the maximum eigenvalue of matrix A defined by

$$A := \sum_{n,m=1}^N \alpha_n |n\rangle \langle m| + (d-1) \sum_{n=1}^N \alpha_n |n\rangle \langle n|, \tag{87}$$

and satisfies the following normalization condition:

$$\left(\sum_{n=1}^N \beta_n \right)^2 + (d-1) \sum_{n=1}^N \beta_n^2 = d. \tag{88}$$

In the above equation, non-negative real parameters $\{\alpha_n\}_{n=1}^N$ represent an asymmetry of the UQC and satisfy $\sum_{n=1}^N \alpha_n = 1$. Equation (86) leads that an output state $|\Psi_O\rangle$ of this UQC protocol corresponding to a given input state $|\psi_I\rangle := \sum_{i=0}^{d-1} a_i |i\rangle$ can be written as

$$|\Psi_O\rangle = \sum_{i,j=0}^{d-1} a_j (\beta_1 |ji \cdots i\rangle + \beta_2 |ij \cdots i\rangle + \cdots + \beta_N |ii \cdots j\rangle). \tag{89}$$

We should note that even if $N = 3$, $U_{I \rightarrow O}$ defined by Equation (86) does not coincide the cloning map given by Equation (10); that is, the UQC protocol of Key et al. is not a straightforward extension of the UQC protocol used in this paper.

Let us assume $d \gg N$, that is, the dimension d of the input space \mathcal{H}_I is much larger than the number of clones N , and give a rough estimation of the communication cost that is necessary to multicast $|\Psi_O\rangle$ to N distinct terminal nodes on quantum networks. Here, we also assume $\alpha_1 > \alpha_n$ for all $n \geq 2$ for simplicity. Under this condition, A can be approximated the diagonal matrix as

$$A \approx (d-1) \sum_{n=1}^N \alpha_n |n\rangle \langle n|. \tag{90}$$

Then, the maximum eigenvector $\{\beta_n\}_{n=1}^N$ of A satisfying Equation (88) can be approximately given by $\beta_1 = 1$ and $\beta_n = 0$ for all $n \geq 2$. Hence, for a given input state $|\psi_I\rangle \in \mathcal{H}_I$, the output state $|\Psi_O\rangle \in \mathcal{H}_O$ can be approximated as

$$|\Psi_O\rangle \approx |\psi_I\rangle \otimes |GHZ_{N-1}\rangle, \tag{91}$$

where $|GHZ_{N-1}\rangle$ is the $N - 1$ partite GHZ state on $(\mathbb{C}^d)^{\otimes N-1}$ defined as

$$|GHZ_{N-1}\rangle := \frac{1}{\sqrt{d}} \sum_{i=0}^{d-1} |ii \cdots i\rangle.$$

Let us consider a quantum network described by an undirected graph G with one source node s and N target nodes t_1, \dots, t_N , and assume that the protocol can multicast a GHZ-type state $\sum_{i=0}^{d-1} a_i |ii \cdots i\rangle$ from the source node to the N target nodes for a given input state $|\psi_I\rangle = \sum_{i=0}^{d-1} a_i |i\rangle$. Now, we consider the similar type of multicast protocol used in this paper. Thus, the protocol consists of the following three steps:

- Step 1** A quantum operation possibly including measurements are applied to $|\psi_I\rangle$ on s , where the measurement result (if they exist) is sent to t_1, \dots, t_N .
- Step 2** The output of the quantum operation, which should be d -dimensional system, is multicast to the target nodes t_1, \dots, t_N by the protocol of Kobayashi et al.
- Step 3** The state $|\Psi_O\rangle$ defined by Equation (89) is constructed by LOCC with an additional entanglement resource on t_1, \dots, t_N .

Now, we give a rough discussion that strongly suggests that the necessary entanglement resource on the target node is $O(\log d)$ ebit: In order to make the state $|\Psi_O\rangle$ given by Equation (89) on the target nodes, the protocol of Kobayashi et al. may be necessary to multicast the whole d -dimensional output space of the quantum operation on s in Step 2. In other words, any quantum state $\sum_{i=0}^{d-1} a'_i |i\rangle$ on \mathbb{C}^d is necessary to multicast by the protocol of Kobayashi et al. from s to t_1, \dots, t_N , where a'_i is not equal to a_i in general. Then, when $a'_0 = 1$ and $a'_i = 0$ for all $i \geq 1$, the output state of the protocol of Kobayashi et al. is a product state $|00 \cdots 0\rangle$. On the other hand, Equation (91) guarantees that when $d \gg N$, the entanglement of the target state $|\Psi_O\rangle$ is $O(\log d)$ ebit for any bipartition on $\{1, \dots, N\}$ except $1|2, \dots, N$. Therefore, we need an additional entanglement resource with an amount of at least $O(\log d)$ ebit for any bipartite except $1|2, \dots, N$.

This conclusion is completely different from the results in Sections 3.1 and 3.2, where $1 \rightarrow 2$ and $1 \rightarrow 3$ asymmetric optimal UQCs are constructed with one use of the protocol of Kobayashi et al. and an entanglement resource, which is a constant with respect to the dimension d . Hence, we conclude that by using existing asymmetric optimal UQC protocol, there might not exist a straightforward extension of our protocol for an arbitrary large number of terminal nodes.

4.4. Summary

In this paper, we considered quantum multicast network coding as the multicasting of optimal UQCs over a quantum network. By extending the results of Owari et al. [48–50] for a multicast of symmetric optimal UQCs, we developed a protocol to multicast asymmetric optimal UQCs over a quantum network. Our results can be summarized as follows. Suppose a quantum network is described by an undirected graph G with one source node and two (three) target nodes, and each quantum channel on the quantum network G can transmit one q -dimensional quantum system in a single session. Furthermore, suppose that there exists a classical solvable multicast network code with source rate r for a classical network described by an acyclic directed graph G' , where G is an undirected underlying graph of G' . We showed that under the above assumptions, our protocol can multicast $1 \rightarrow 2$ ($1 \rightarrow 3$) asymmetric optimal UQCs of a q^r -dimensional state from the source node to

the target nodes by consuming a small amount of entanglement that does not scale with q , which is shared among the target nodes. We further showed that our protocol can be used for efficient preparation of quantum telecloning over a quantum network.

As we have discussed in the previous subsection, when we use a known scheme of a $1 \rightarrow N$ asymmetric optimal UQC for $N \geq 4$, a protocol which derived straightforward extension of our scheme need $O(\log d)$ ebits shared among target nodes. Thus, the extension of our protocol for $1 \rightarrow n$ asymmetric optimal UQCs for $n \leq 4$ is not so straightforward. Hence, we leave this study as our future work.

In this paper, we assumed that all quantum channels on a quantum network are noiseless. This assumption can be justified by considering our protocol as a protocol on the layer on which error correction has been already implemented. However, as is well known, such complete error correction of a quantum channel is beyond the present technology. For example, the long-distance distribution of GHZ-type states, which is nothing but the purpose of the protocol of Kobayashi et al., is a huge challenge in quantum networks. We note that as a practical protocol for this purpose, recently, a protocol to distribute the postselected GHZ state by using entanglement swapping is proposed [106].

As we have mentioned above, in this paper, we assume that error correction of quantum channels has been applied on a quantum network before our protocol is implemented. In other words, we assume that optimization is applied separately on these two layers. On the other hand, if we optimize these two layers simultaneously, we may derive a better protocol. We leave this study as future work.

The protocol of Kobayashi et al., which is one of the main subroutines of our protocol, gives an efficient protocol to share GHZ states. On the other hand, as we have explained in Section 1, except GHZ-states, there are many classes of multipartite entangled states that are incomparable to the class of GHZ states under SLOCC-like W states, Dicke states (generalized W states), etc. It may be desirable to find an efficient quantum network protocol to share these classes of states. This may be also our future work.

Author Contributions: Conceptualization, M.O.; methodology, M.O.; validation, M.O.; investigation, Y.H. and M.O.; writing—original draft preparation, Y.H.; writing—review and editing, M.O.; visualization, Y.H. and M.O.; supervision, M.O.; project administration, M.O.; funding acquisition, M.O. All authors have read and agreed to the published version of the manuscript.

Funding: This research was funded by the JSPS Kakenhi (C) No. 16K00014, No. 17K05591, No. 20K03779, and No. 21K03388.

Institutional Review Board Statement: Not applicable.

Data Availability Statement: Not applicable.

Conflicts of Interest: The authors declare no conflict of interest.

References

1. Preskill, J. Quantum computing in the nisq era and beyond. *Quantum* **2018**, *2*, 79. [[CrossRef](#)]
2. Arute, F.; Arya, K.; Babbush, R.; Bacon, D.; Bardin, J.C.; Barends, R.; Biswas, R.; Boixo, S.; Brandao, F.G.S.L.; Buell, D.A.; et al. Quantum supremacy using a programmable superconducting processor. *Nature* **2019**, *574*, 505–510. [[CrossRef](#)] [[PubMed](#)]
3. Pednault, E.; Gunnels, J.A.; Nannicini, G.; Horesh, L.; Wisnieff, R. Leveraging secondary storage to simulate deep 54-qubit sycamore circuits. *arXiv* **2019**, arXiv:1910.09534.
4. Liu, Y.; Liu, X.; Li, F.; Fu, H.; Yang, Y.; Song, J.; Zhao, P.; Wang, Z.; Peng, D.; Chen, H.; et al. Closing the “Quantum Supremacy” Gap: Achieving Real-Time Simulation of a Random Quantum Circuit Using a New Sunway Supercomputer. In Proceedings of the SC '21: Proceedings of the International Conference for High Performance Computing, Networking, Storage and Analysis, St. Louis, MO, USA, 14–19 November 2021; pp. 1–12.
5. Biamonte, J.; Wittek, P.; Pancotti, N.; Rebentrost, P.; Wiebe, N.; Lloyd, S. Quantum Machine Learning, *Nature* **2017**, *549*, 195–202. [[CrossRef](#)]
6. Havlíček, V.; Córcoles, A.D.; Temme, K.; Harrow, A.W.; Kandala, A.; Chow, J.M.; Gambetta, J.M. Supervised learning with quantum-enhanced feature spaces, *Nature* **2019**, *567*, 209–212. [[CrossRef](#)]
7. Cerezo, M.; Arrasmith, A.; Babbush, R.; Benjamin, S.C.; Endo, S.; Fujii, K.; McClean, J.R.; Mitarai, K. Yuan, X.; Cincio, L.; et al. Variational quantum algorithms, *Nat. Rev. Phys.* **2021**, *3*, 625–644.

8. Bharti, K.; Cervera-Lierta, A.; Kyaw, T.H.; Haug, T.; Alperin-Lea, S.; Anand, A.; Degroote, M.; Heimonen, H.; Kottmann, J.S.; Menke, T.; et al. Noisy intermediate-scale quantum algorithms, *Rev. Mod. Phys.* **2022**, *94*, 015004. [[CrossRef](#)]
9. Zhou, M.-G.; Cao, X.-Y.; Lu, Y.-S.; Wang, Y.; Bao, Y.; Jia, Z.-Y.; Fu, Y.; Yin, H.-L.; Chen, Z.-B. Experimental Quantum Advantage with Quantum Coupon Collector. *Research* **2022**, *2022*, 9798679. [[CrossRef](#)]
10. Peruzzo, A.; McClean, J.; Shadbolt, P.; Yung, M.-H.; Zhou, X.-Q.; Love, P. J. Aspuru-Guzik, A.; O'Brien, J.L. A variational eigenvalue solver on a photonic quantum processor. *Nat. Commun.* **2014**, *5*, 4213. [[CrossRef](#)]
11. O'Malley, P.J.J.; Babbush, R.; Kivlichan, I.D.; Romero, J.; McClean, J.R.; Barends, R.; Kelly, J.; Roushan, P.; Tranter, A.; Ding, N.; et al. Scalable Quantum Simulation of Molecular Energies. *Phys. Rev. X* **2016**, *6*, 031007. [[CrossRef](#)]
12. Cao, Y.; Romero, J.; Olson, J.P.; Degroote, M.; Johnson, P.D.; Kieferová, M.; Kivlichan, I.D.; Menke, T.; Peropadre, B.; Sawaya, N.P.D.; et al. Quantum Chemistry in the Age of Quantum Computing. *Chem. Rev.* **2019**, *119*, 10856–10915. [[CrossRef](#)]
13. McArdle, S.; Endo, S.; Aspuru-Guzik, A.; Benjamin, S.C.; Yuan, X. Quantum computational chemistry. *Rev. Mod. Phys.* **2020**, *92*, 015003. [[CrossRef](#)]
14. Arute, F.; Arya, K.; Babbush, R.; Bacon, D.; Bardin, J.C.; Barends, R.; Boixo, S. Hartree-Fock on a superconducting qubit quantum computer. *Science* **2020**, *369*, 1084–1089.
15. Kawachi A.; Koshihara, T. Progress in quantum computational cryptography. *J. Univ. Comput. Sci.* **2006**, *12*, 691–709.
16. Broadbent, A.; Fitzsimons, J.; Kashefi, E. Universal blind quantum computation. In Proceedings of the 50th Annual IEEE Symposium on Foundation of Computational Science, Washington, DC, USA, 25–27 October 2009; pp. 517–526.
17. Morimae T.; Fujii, K. Blind quantum computation protocol in which alice only makes measurements. *Phys. Rev. A* **2013**, *87*, 050301. [[CrossRef](#)]
18. Wiesner, S. Conjugate Coding. *SIGACT News* **1983**, *15*, 78–88. [[CrossRef](#)]
19. Aaronson, S. Quantum Copy-Protection and Quantum Money. In Proceedings of the 24th Annual IEEE Conference on Computational Complexity, Paris, France, 15–18 July 2009; pp. 229–242.
20. Van Meter, R. *Quantum Networking*; Wiley: Hoboken, NJ, USA, 2014.
21. Kimble, H.J. The quantum internet. *Nature* **2008**, *453*, 1023–1030. [[CrossRef](#)]
22. Wehner, S.; Elkouss, D.; Hanson, R. Quantum internet: A vision for the road ahead. *Science* **2018**, *362*, eaam9288. [[CrossRef](#)]
23. Acín, A.; Cirac, J.; Lewenstein, M. Entanglement percolation in quantum networks. *Nat. Phys.* **2007**, *3*, 256–259. [[CrossRef](#)]
24. Pirandola, S.; Laurenza, R.; Ottaviani, C.; Banchi, L. Fundamental limits of repeaterless quantum communications. *Nat. Commun.* **2017**, *8*, 15043. [[CrossRef](#)]
25. Rigovacca, L.; Kato, G.; Bäuml, S.; Kim, M.S.; Munro, W.J.; Azuma, K. Versatile relative entropy bounds for quantum networks. *New J. Phys.* **2018**, *20*, 013033. [[CrossRef](#)]
26. Pirandola, S. End-to-end capacities of a quantum communication network. *Commun. Phys.* **2019**, *2*, 51. [[CrossRef](#)]
27. Hahn, F.; Pappa, A.; Eisert, J. Quantum network routing and local complementation. *NPJ Quant. Inf.* **2019**, *5*, 76. [[CrossRef](#)]
28. Bäuml, S.; Azuma, K.; Kato, G.; Elkouss D. Linear programs for entanglement and key distribution in the quantum internet. *Commun. Phys.* **2020**, *3*, 55. [[CrossRef](#)]
29. Hahn, F.; Dahlberg, A.; Eisert, J.; Pappa, A. Limitations of nearest-neighbour quantum networks. *arXiv* **2022**, arXiv:2202.10886.
30. Flamini, F.; Spagnolo, N.; Sciarrino, F. Photonic quantum information processing: A review. *Rep. Prog. Phys.* **2018**, *82*, 016001. [[CrossRef](#)]
31. Pompili, M.; Hermans, L.N.; Baier, S.; Beukers, H.K.C.; Humphreys, P.C.; Schouten, R.N.; Vermeulen, R.F.; Tiggelman, M.J.; dos Santos Martins, L.; Dirkse, B.; et al. Realization of a multinode quantum network of remote solid-state qubits. *Science* **2021**, *372*, 259–264. [[CrossRef](#)]
32. Briegel, H.-J.; Dür, W.; Cirac, J.I.; Zoller, P. Quantum Repeaters: The Role of Imperfect Local Operations in Quantum Communication. *Phys. Rev. Lett.* **1998**, *81*, 5932. [[CrossRef](#)]
33. Duan, L.-M.; Lukin, M.D.; Cirac, J.I.; Zoller, P. Long-distance quantum communication with atomic ensembles and linear optics. *Nature* **2001**, *414*, 413–418. [[CrossRef](#)] [[PubMed](#)]
34. Tanenbaum, A.S.; Feamster, N.; Wetherall, D.J. *Computer Networks*, 6th ed.; Pearson: London, UK, 2021.
35. Horodecki, R.; Horodecki, P.; Horodecki, M.; Horodecki, K. Quantum entanglement. *Rev. Mod. Phys.* **2009**, *81*, 865–942. [[CrossRef](#)]
36. Dür, W.; Vidal, G.; Cirac, J.I. Three qubits can be entangled in two inequivalent ways. *Phys. Rev. A* **2000**, *62*, 062314. [[CrossRef](#)]
37. Ho, T.; Lun, D.S. *Network Coding: An Introduction*; Cambridge University Press: Cambridge, UK, 2008.
38. Yeung, R.W. *Information Theory and Network Coding*; Springer: Berlin/Heidelberg, Germany, 2008.
39. Ahlswede, R.; Cai, N.; Li, S.-Y.R.; Yeung, R.W. Network information flow. *IEEE Trans. Inf. Theor.* **2000**, *46*, 1204–1216. [[CrossRef](#)]
40. Hayashi, M.; Iwama, K.; Nishimura, H.; Raymond, R.; Yamashita, S. Quantum Network Coding. In Proceedings of the STACS 2007 SE-52, Aachen, Germany, 22–24 February 2007; Lecture Notes in Computer Science; Thomas, W., Weil, P., Eds.; Springer: Berlin/Heidelberg, Germany, 2007; Volume 4393, pp. 610–621.
41. Hayashi, M. Prior entanglement between senders enables perfect quantum network coding with modification. *Phys. Rev. A* **2007**, *76*, 40301. [[CrossRef](#)]
42. Shi, Y.; Soljanin, E. On multicast in quantum networks. In Proceedings of the 40th Annual Conference on Information Sciences and Systems, Princeton, NJ, USA, 22–24 March 2006; pp. 871–876.

43. Kobayashi, H.; Le Gall, F.; Nishimura, H.; Rötteler, M. General Scheme for Perfect Quantum Network Coding with Free Classical Communication. In Proceedings of the ICALP 2009: Automata, Languages and Programming, Rhodes, Greece, 5–12 July 2009; Lecture Notes in Computer Science; Albers, S., Marchetti-Spaccamela, A., Matias, Y., Nikolettseas, S., Thomas, W., Eds.; Springer: Berlin/Heidelberg, Germany, 2009; Volume 5555, pp. 622–633.
44. Kobayashi, H.; Le Gall, F.; Nishimura, H.; Rötteler, M. Perfect quantum network communication protocol based on classical network coding. In Proceedings of the 2010 IEEE International Symposium on Information Theory (ISIT), Austin, TX, USA, 13–18 June 2010; pp. 2686–2690.
45. Leung, D.; Oppenheim, J.; Winter, A. Quantum Network Communication; The Butterfly and Beyond. *IEEE Trans. Inf. Theory* **2010**, *56*, 3478–3490. [[CrossRef](#)]
46. Kobayashi, H.; Le Gall, F.; Nishimura, H.; Rotteler, M.; Constructing quantum network coding schemes from classical nonlinear protocols. In Proceedings of the 2011 IEEE International Symposium on Information Theory (ISIT), St. Petersburg, Russia, 31 July–5 August 2011; pp. 109–113.
47. Jain, A.; Franceschetti, M.; Meyer, D.A. On quantum network coding. *J. Math. Phys.* **2011**, *52*, 032201. [[CrossRef](#)]
48. Owari, M.; Kato, G.; Murao, M. Multicast Quantum Network Coding on the Butterfly Network. JP2013-201654A, 3 October 2013. (In Japanese)
49. Kato, G.; Owari, M.; Murao, M. Multicast Quantum Network Coding. JP2014-192875A, 6 October 2014. (In Japanese)
50. Kato, G.; Owari, M.; Murao, M. Multicast Quantum Network Coding. JP2015-220621A, 7 December 2015. (In Japanese)
51. Li, J.; Chen, X.-B.; Xu, G.; Yang Y.-X.; Li, Z.-P. Perfect Quantum Network Coding Independent of Classical Network Solutions. *IEEE Commun. Lett.* **2015**, *19*, 115–118. [[CrossRef](#)]
52. Xu, G.; Chen X.-B.; Li, J.; Wang, C.; Yang, Y.-X.; Li, Z. Network coding for quantum cooperative multicast. *Quant. Inf. Process.* **2015**, *14*, 4297–4322. [[CrossRef](#)]
53. Epping, M.; Kampermann, H.; Bruß, D. Quantum Router with Network Coding. *New J. Phys.* **2006**, *18*, 103052. [[CrossRef](#)]
54. Li, J.; Chen, X.; Sun, X.; Li, Z.; Yang, Y. Quantum network coding for multi-unicast problem based on 2D and 3D cluster states. *Sci. China Inf. Sci.* **2016**, *59*, 042301. [[CrossRef](#)]
55. Li, D.D.; Gao, F.; Qin, S.J.; Wen, Q.-Y. Perfect quantum multiple-unicast network coding protocol. *Quant. Inf. Process.* **2018**, *17*, 13. [[CrossRef](#)]
56. Pan, X.-B.; Xu, G.; Li, Z.-P.; Chen, X.-B.; Yang, Y.-X. Quantum network coding without loss of information. *Quant. Inf. Process.* **2021**, *20*, 65. [[CrossRef](#)]
57. Pan, X.-B.; Chen, X.-B.; Xu, F.; Dou, Z.; Li, Z.-P.; Yang, Y.-X. Quantum multicast communication over the butterfly network. *Chin. Phys. B* **2022**, *31*, 010305. [[CrossRef](#)]
58. Owari, M.; Kato, G.; Hayashi, M. Secure Quantum Network Coding on Butterfly Network. *Quant. Sci. Technol.* **2017**, *3*, 014001. [[CrossRef](#)]
59. Kato, G.; Owari, M.; Hayashi, M. Single-Shot Secure Quantum Network Coding for General Multiple Unicast Network With Free One-Way Public Communication. *IEEE Trans. Inf. Theor.* **2021**, *67*, 4564–4587. [[CrossRef](#)]
60. Song, S.; Hayashi, M. Quantum Network Code for Multiple-Unicast Network with Quantum Invertible Linear Operations. In Proceedings of the 13th Conference on the Theory of Quantum Computation, Communication and Cryptography (TQC 2018), Sydney, Australia, 16–18 July 2018.
61. Song, S.; Hayashi, M. Secure Quantum Network Code without Classical Communication, *IEEE Trans. Inf. Theor.* **2020**, *66*, 1178–1192. [[CrossRef](#)]
62. Shang, T.; Zhang, Y.; Liu, R.; Liu, J. Quantum network coding reducing decoherence effect. *Quant. Inf. Process.* **2021**, *20*, 267. [[CrossRef](#)]
63. Satoh, T.; Ishizaki, K.; Nagayama, S.; Van Meter, R. Analysis of Quantum Network Coding for Realistic Repeater Networks. *Phys. Rev. A* **2016**, *93*, 032302. [[CrossRef](#)]
64. Matsuo, T.; Satoh, T.; Nagayama, S.; Van Meter, R. Analysis of Measurement-based Quantum Network Coding over Repeater Networks under Noisy Conditions. *Phys. Rev. A* **2018**, *97*, 062328. [[CrossRef](#)]
65. Akibue, S.; Murao, M. Network coding for distributed quantum computation over cluster and butterfly networks. *IEEE Trans. Inf. Theor.* **2016**, *62*, 6620–6637. [[CrossRef](#)]
66. Lu, H.; Li, Z.-D.; Yin, X.-F.; Zhang, R.; Fang, X.-X.; Li, L.; Liu, N.-L.; Xu, F.; Chen, Y.-A.; Pan, J.-W. Experimental Quantum Network Coding. *NPJ Quant. Inf.* **2019**, *5*, 1–5. [[CrossRef](#)]
67. Pathumsoot, P.; Matsuo, T.; Satoh, T.; Hajdušek, M.; Suwanna, S.; Van Meter, R. Modeling of measurement-based quantum network coding on a superconducting quantum processor. *Phys. Rev. A* **2020**, *101*, 052301. [[CrossRef](#)]
68. Traskov, D.; Ratnakar, N.; Lun, D.S.; Koetter, R.; Medard, M. Network Coding for Multiple Unicasts: An Approach based on Linear Optimization. In Proceedings the of 2006 IEEE International Symposium on Information Theory (ISIT2006), Washington, DC, USA, July 9–14. 2006; pp. 1758–1762.
69. Wootters, W.K.; Zurek, W.H. A single quantum cannot be clone. *Nature* **1982**, *299*, 802–833. [[CrossRef](#)]
70. Scarani, V.; Iblisdir, S.; Gison, N. Quantum cloning. *Rev. Mod. Phys.* **2005**, *77*, 1225–1256. [[CrossRef](#)]
71. Fan, H.; Wang, Y.-N.; Jing, L.; Yue, J.-D.; Shi, H.-D.; Zhang, Y.-L.; Mu, L.-Z. Quantum cloning machines and the applications. *Phys. Rep.* **2014**, *544*, 241–322. [[CrossRef](#)]
72. Buzek, V.; Hillery, M. Quantum copying: Beyond the no-cloning theorem. *Phys. Rev. A* **1996**, *54*, 1844. [[CrossRef](#)]

73. Gisin, N.; Massar, S. Optimal Quantum Cloning Machines. *Phys. Rev. Lett.* **1997**, *79*, 2153. [[CrossRef](#)]
74. Werner, R.F. Optimal cloning of pure states. *Phys. Rev. A* **1998**, *58*, 1827. [[CrossRef](#)]
75. Niu, C.-S.; Griffiths, R.B. Optimal copying of one quantum bit. *Phys. Rev. A* **1998**, *58*, 4377. [[CrossRef](#)]
76. Cerf, N.J. Asymmetric quantum cloning machines. *Acta Phys. Slov.* **1998**, *48*, 115.
77. Buzek, V.; Hillery, M.; Bednik, R. Controlling the flow of information in quantum cloners: Asymmetric cloning. *Acta Phys. Slov.* **1998**, *48*, 177–184.
78. Cerf, N.J. Asymmetric quantum cloning in any dimension. *J. Mod. Opt.* **2000**, *47*, 187–209. [[CrossRef](#)]
79. Fiurasek, J.; Filip, R.; Cerf, N.J. Highly asymmetric quantum cloning in arbitrary dimension. *Quant. Inform. Comp.* **2005**, *5*, 583.
80. Iblisdir, S.; Acín, A.; Cerf, N.J.; Filip, R.; Fiurášek, J.; Gisin, N. Multipartite asymmetric quantum cloning. *Phys. Rev. A* **2005**, *72*, 042328. [[CrossRef](#)]
81. Key, A.; Kaszlikowski, D.; Ramanathan, R. Optimal Cloning and Singlet Monogamy. *Phys. Rev. Lett.* **2009**, *103*, 050501. [[CrossRef](#)]
82. Ren, X.-J.; Xiang, Y.; Fan, H. Optimal asymmetric $1 \rightarrow 4$ quantum cloning in arbitrary dimension. *Eur. Phys. J. D* **2011**, *65*, 621–625. [[CrossRef](#)]
83. Ćwikliński, P.; Horodecki, M.; Studziński, M. Region of fidelities for $1 \rightarrow N$ universal qubit quantum cloner. *Phys. Lett. A* **2012**, *376*, 2178–2187. [[CrossRef](#)]
84. Key, A.; Ramanathan, R.; Kaszlikowski, D. Optimal Asymmetric Quantum Cloning. *Quant. Inf. Comput.* **2013**, *13*, 880.
85. Xiao, X.; Yao, Y.; Zhou, L.M.; Wang, X. Distribution of quantum Fisher information in asymmetric cloning machines. *Sci. Rep.* **2014**, *4*, 7361. [[CrossRef](#)] [[PubMed](#)]
86. Lamas-Linares, A.; Simon, C.; Howell, J.C.; Bouwmeester, D. Experimental Quantum Cloning of Single Photons. *Science* **2002**, *296*, 712. [[CrossRef](#)]
87. Irvine, W.T.M.; Linares, A.L.; de Dood, M.J.A.; Bouwmeester, D. Optimal Quantum Cloning on a Beam Splitter. *Phys. Rev. Lett.* **2004**, *92*, 047902. [[CrossRef](#)] [[PubMed](#)]
88. Andersen, U.L.; Josse, V.; Leuchs, G. Unconditional Quantum Cloning of Coherent States with Linear Optics. *Phys. Rev. Lett.* **2005**, *94*, 240503. [[CrossRef](#)]
89. Zhao, Z.; Zhang, A.-N.; Zhou, X.-Q.; Chen, Y.-A.; Lu, C.-Y.; Karlsson, A.; Pan, J.-W. Experimental Realization of Optimal Asymmetric Cloning and Telecloning via Partial Teleportation. *Phys. Rev. Lett.* **2005**, *95*, 030502. [[CrossRef](#)]
90. Sabuncu, M.; Leuchs, G.; Andersen, U.L. Experimental continuous-variable cloning of partial quantum information. *Phys. Rev. A* **2008**, *78*, 052312. [[CrossRef](#)]
91. Nagali, E.; Sansoni, L.; Sciarrino, F.; De Martini, F.; Marrucci, L.; Piccirillo, B.; Karimi, E.; Santamato, E. Optimal quantum cloning of orbital angular momentum photon qubits through Hong–Ou–Mandel coalescence. *Nat. Photon.* **2009**, *3*, 720–723. [[CrossRef](#)]
92. Bechmann-Pasquinucci, H.; Gisin, N. Incoherent and coherent eavesdropping in the six-state protocol of quantum cryptography. *Phys. Rev. A* **1999**, *59*, 4238. [[CrossRef](#)]
93. Bruß, D.; Macchiavello, C. Optimal Eavesdropping in Cryptography with Three-Dimensional Quantum States. *Phys. Rev. Lett.*, **2002**, *88*, 127901. [[CrossRef](#)]
94. Cerf, N.J.; Bourennane, M.; Karlsson, A.; Gisin, N. Security of Quantum Key Distribution Using d-Level Systems. *Phys. Rev. Lett.* **2002**, *88*, 127902. [[CrossRef](#)]
95. Acín, A.; Gisin, N.; Scarani, V. Coherent pulse implementations of quantum cryptography protocols resistant to photon number splitting attacks. *Phys. Rev. A* **2004**, *69*, 012309. [[CrossRef](#)]
96. Xiong, Z.-X.; Shi, H.-D.; Wang, Y.-N.; Jing, L.; Lei, J.; Mu, L.-Z.; Fan, H. General quantum key distribution in higher dimension. *Phys. Rev. A* **2012**, *85*, 012334. [[CrossRef](#)]
97. Sharma, U.K.; Chakrabarty, I.; Shukla, M.K. Broadcasting quantum coherence via cloning. *Phys. Rev. A* **2017**, *96*, 052319. [[CrossRef](#)]
98. Kato, G.; Murao, M.; Owari, M. Multicast quantum network coding as optimal cloning over a quantum network. 2022, *in preparation*.
99. Ghiu, I. Asymmetric quantum telecloning of d-level systems and broadcasting of entanglement to different locations using the “many-to-many” communication protocol. *Phys. Rev. A* **2003**, *67*, 012323. [[CrossRef](#)]
100. Chen, L.; Chen, Y.-X. Asymmetric quantum telecloning of multiqubit states. *Quant. Inf. Comp.* **2007**, *7*, 716–729.
101. Hayashi, M. *Group Representation for Quantum Theory*; Springer: Berlin/Heidelberg, Germany, 2017.
102. Bennett, C.H.; Brassard, G.; Crépeau, C.; Jozsa, R.; Peres, A.; Wootters, W.K. Teleporting an unknown quantum state via dual classical and Einstein-Podolsky-Rosen Channels. *Phys. Rev. Lett.* **1993**, *70*, 1895. [[CrossRef](#)]
103. Murao, M.; Jonathan, D.; Plenio, M.B.; Vedral, V. Quantum telecloning and multiparticle entanglement. *Phys. Rev. A* **1999**, *59*, 156–161. [[CrossRef](#)]
104. Murao, M.; Plenio, M.B.; Vedral, V. Quantum-information distribution via entanglement. *Phys. Rev. A* **2000**, *61*, 032311. [[CrossRef](#)]
105. Dür, W.; Cirac, J.I. Multiparty teleportation. *J. Mod. Opt.* **2000**, *47*, 247–255. [[CrossRef](#)]
106. Fu, Y.; Yin, H.-L.; Chen, T.-Y.; Chen, Z.-B. Long-Distance Measurement-Device-Independent Multiparty Quantum Communication. *Phys. Rev. Lett.* **2015**, *114*, 090501. [[CrossRef](#)]